



Design and Manufacture of a Pick-and-Place Manipulator for Integration within an Autonomous Underwater Vehicle

Submitted by Tan Hui Juan Esther (A0100874L)

Department of Mechanical Engineering

In partial fulfillment of the requirements for the Degree of Bachelor of Engineering

National University of Singapore

Session 2015/2016

Summary

Underwater manipulation systems make it possible to access and perform mechanical works in hostile and hazardous environments where humans cannot enter, such as the deep oceans, icy waters, natural disaster region or a man-made wreckage. They are highly sought after in industries ranging from the Oil and Gas Industry to Search and Recovery, Deep water Archaeology and Marine Science, where they are required to perform tasks such as welding, valve turning and connector plugging, retrieval of fragile corals or recovery of free-floating objects (Ridao, Carreras, Ribas, Sanz, & Oliver, n.d.).

These manipulation systems are typically installed on board an underwater vehicle, notably a Remotely Operated Vehicle (ROV) where tasks are mainly performed under human supervision, or an Autonomous Underwater Vehicle (AUV) where tasks are performed independently of human control. Today's manipulator systems swings between the extremes of being either too heavy and expensive (Cooney, 2006), or too simple and lacking in functionalities. Also, the multi-purpose usage of manipulators in various facets demands for a robust and versatile gripping system.

Henceforth, this project will be on the research, design and fabrication of a manipulator, which serves a dual role of meeting the industry needs in manipulation systems and also for competitive use on the Bumblebee Autonomous Underwater Vehicle (AUV). In this thesis, the mechanical design and integration of a manipulator is presented, with versatile gripping achieved using a Jamming Gripper technique and precise positioning achieved via pneumatic actuations and high torque servo rotation.

Acknowledgements

I would like to extend my heartfelt appreciation and gratitude to the following people who have made this FYP possible:

Firstly I would like to give my glory and thanks to God, my Lord Jesus Christ, in whom all things are made possible, who is ever-present in good times and bad times, who delivers me from troubles and difficulties, who has been my source of comfort, strength and wisdom;

Next, my supervisor, Professor Marcelo Ang, first for supporting this self-initiated project, then for providing valuable advice and support throughout this journey which has really taught me a lot and provided me the hands-on exposure I desired as an engineer;

Thank you to Festo for sponsoring the Pneumatic Accessories, Cititech for Laser-Cut Parts and Industrial partners for their words of advice and encouragement – Wan Chern from Festo, Versaball CTO John Amend;

Thank you Lab Techs from Control Lab – Mrs Ooi, Mdm Hamidah Mr Sakthi, & from FSC – Dickson, Mr Tan;

My Bumblebee teammates who made this project possible, esp Grace, KeeYeow, EngWei, AlexJohn, Steven, AlexFoo, QiXiang, Vanessa, ShihChiang, JunJie, Jin. I can never thank you enough for your support, guidance, advice & help with diving. JiaMing, RenJie, Ruth for helping me along the way with ideas on servo management or video-taking. Big thanks to Ren Zhi, who took up the design of the electrical architecture of the arm, for not giving up, for your jovial nature and for your companionship over those late nights or long weekends in lab;

My wonderful CG who prayed for my projects, consisting of JinZaw, Emily, Beatrice, Rachel, Elissa, Faye, Angeline, Audrey, Dora, Wesley, Joshua, Nigel, and Eleanor the ex-neighbour's neighbour for praying too;

My fellow aunties Amanda, Pei Ying, Audrey – the people who made me look forward to coming to school;

Awesome Friends who have prayed for me or offered a kind word along the way;

Last but not the least, my dear family - Dad, Mum, Dajie, Erjie for your love, care, prayers, encouragement, patience, and support. For being a huge part of my life. Thank you.

Table of Contents

Summary.....	i
Acknowledgements	ii
Table of Contents	iii
List of Figures.....	vi
List of Tables	xiii
1. Introduction	1
1.1. Objectives	1
1.2. Problem Statement.....	1
1.3. Scope.....	3
1.3.1. Design Constraints.....	3
1.3.2. Competition Manipulator Tasks	5
2. Literature Survey.....	6
2.1. Manipulator Arm Types.....	6
2.2. End-effector Types	6
2.2.1. Universal Jamming gripper technique using granular material.....	7
3. Mechanical Design of End-effector	12
3.1. Components of the Jamming Gripper	12
3.2. Pre-experiment.....	12
3.3. End-effector Design.....	16

3.3.1.	End-effector Design 1	16
3.3.2.	End-effector Design 2	19
3.4.	Fabrication and Testing	21
3.4.1.	Testing in Air	22
3.4.2.	Testing in Water	24
4.	Mechanical Design of Manipulator Arm	26
4.1.	Design 1	26
4.1.1.	Limitations of Design 1	29
4.2.	Design 2	30
4.2.1.	Enhancements to Design 2	31
4.2.2.	Limitations of Design 2.5	33
4.3.	Design 3	34
4.3.1.	Finite Element Analysis (FEA)	41
4.3.2.	Computational Fluid Dynamics (CFD)	45
5.	Electrical Architecture of Manipulator	50
6.	Assembly and Testing of Manipulator	51
6.1.	Testing in Air	51
6.2.	Testing in water	52
7.	Results and Discussions	53
8.	Conclusions	55

9. Recommendations for Future Works	56
Appendices	57
Appendix 2.....	58
References	77

List of Figures

Figure 1: Bumblebee Autonomous Underwater Vehicle Version 3.0.....	1
Figure 2: Industry Underwater Manipulators; Left - Schilling Robotics TITAN 4 (FMC Technologies, 2015), Right- Seabotix Grabber on Remotely Operated Vehicle (Seabotix, 2015).....	2
Figure 3: 3D CAD of Manipulator Design for Bumblebee AUV Version 2.5.....	2
Figure 4: CAD of Available Mounting Space for Manipulator on Bumblebee AUV marked by red box	4
Figure 5: Left - Lack of available space at the Bottom due to the Doppler Velocity Log Sensor, Right -Lack of available space at the Front due to occupancy by the Front Camera, Sonar, and Yaw Thrusters	4
Figure 6: Examples of Manipulation Tasks at the AUV Competitions.....	5
Figure 7: Empire Robotics' VERSABALL Gripper Conforming to Shape and Lifting Objects; Left - Hammer, Right - Brick, (Empire Robotics, 2016)	7
Figure 8: Granular interaction in unjammed (fluid-like) and jammed (solid-like) states (Mozeika, 2015)	8
Figure 9: Contact Networks in the Modeled System; Left - Unjammed state (Packing = 89%) , Right - Jammed state (Packing = 90.5%) state. For each grain, i, a line is drawn from its center to the neighboring grain (Herman, 2013)	9
Figure 10: Left - Features of the Vacuum generator, Right - Bernoulli's Equation (Hyperphysics, 2015)	9

Figure 11: Three gripping modes of Jamming Grippers, Left -Static friction from surface contact, Centre - Geometric constraints from interlocking, Right - Vacuum suction from airtight seal, (Amend et al, 2012)	11
Figure 12: Jamming Gripper Mini Experimental Set-up.....	13
Figure 13: Left - Fine Grain Coffee enables relatively higher object conformation, Centre – Coarse coffee enables relatively lower object conformation, Right – Fine & Coarse Grain Mix enables relatively higher object conformation.....	14
Figure 14: Left – Fine Grain Coffee leaving relatively Less Defined Imprint on membrane, Centre - Coarse Grain Coffee leaving relatively More Defined Imprint on membrane, Right – Fine & Coarse Grain Mix leaving relatively More Defined Imprint on membrane.....	15
Figure 15: Gripper Collar assembly consisting of cup and throat	16
Figure 16: 3-D printed prototypes of Gripping cups - Deep cup versus Shallow wide cup.....	17
Figure 17: Assembly of End-effector	17
Figure 18: Left - Vacuum Pump is connected to the 24” gripper via Custom-made adaptor, Centre - Jamming Gripper is successful in picking up the oval metal structure, Right - Jamming Gripper is successful in picking up the K’nex	18
Figure 19: Partially Exploded CAD View of Pneumatic Housing	18
Figure 20: Left - Isometric CAD View of the Vacuum Generator Mount, Right - CAD Assembly of the Vacuum Generator inside the Pneumatic Hull	19
Figure 21: Left - Cross-sectional CAD of End-effector Design 2; Right - Water Entry Points of End-effector.....	20
Figure 22: CAD Diagram of Gripper Lid Support	20

Figure 23: Left - 3-D Printed ABS Prototype of Design 2 End-Effector, Right - End-effector Assembly comprising 3D printed Gripping Collar, Latex Balloon, Coffee Powder and Filter Paper	21
Figure 24: Left - End-effector lifting up a PVC pipe structure of weight 475g, Right - Weight of PVC pipe structure	21
Figure 25: Left - Gripper Collar, Right - Gripper Lid	22
Figure 26: Setup of Jamming Gripper Experiment in Air	22
Figure 27: 100% gripping success case, Left – Gripper contacts ground (Flat underneath), Right - $\frac{3}{4}$ or more wrap-around Diameter	23
Figure 28: 80% Gripping Success Case from Geometric Interlocking with $\frac{1}{2}$ or less wrap-around Diameter	23
Figure 29: 20% gripping success case, Left– Gripper does not contact ground (Round underneath), Right - $\frac{1}{2}$ or less wrap-around Diameter	24
Figure 30: Experimental Setup for testing Jamming Gripper in Water.....	25
Figure 31: Irregular Object Conformability of Jamming Gripper of a smaller, less packed membrane	25
Figure 32: Successful Gripping using Jamming Gripper of larger, more highly packed membrane	26
Figure 33: CAD model of Manipulator Design in a Keeping Position	28
Figure 34: Left - CFFAP6-16 Cam Follower (Misumi, 2016), Right - Cross-section of a cam follower (Ikont.co.jp, 2016).....	28
Figure 35: Servocity Flanged shaft hub (Servocity.com, 2016).....	28

Figure 36: Manipulator Configurations - Keeping, Forward, Scooping, Picking, Downward positions.....	29
Figure 37: Manipulator Configurations on AUV- Keeping, Forward, Scooping, Picking, Downward	29
Figure 38: CAD model of Manipulator Design in a Forward Extend Position.....	31
Figure 39: Manipulator Configurations on AUV- Forward, Downward and Keeping Positions	31
Figure 40: Working Principle of Festo Semi-Rotary Pneumatic Actuator (Festo, 2015)	32
Figure 41: CAD model of Enhanced Manipulator Design 2.5 in a Forward Extend Position .	32
Figure 42: Manipulator Configurations mounted on AUV- Forward, Downward and Keeping Positions	33
Figure 43: Non-uniform Diameter in Guide Rod Passages within Linear Actuator	33
Figure 44: CAD model of Manipulator Design 3 in a Forward Retracted Position.....	34
Figure 45: Manipulator Configurations mounted on AUV- Forward, Downward and Keeping Positions	35
Figure 46: Gear Relationship (DesignAerospace, 2016).....	35
Figure 47: Left - Optek Slotted Optocoupler (RS Components, 2016), Right - Basic Limit Switch (Omron, 2016)	36
Figure 48: CAD Model of Optocoupler Mount and Limit Switch Mount	37
Figure 49: Servo Setup with a 5:1 Gear Ratio to Step Up the Torque	37
Figure 50: CAD model of Servo Housing	38
Figure 51: CAD model of Servo Housing Lid and Rotary Seal Cap	39
Figure 52: Field of View of a Camera (longrangecamera.com, 2015).....	40

Figure 53: Top - CAD of Forward Manipulator Position within the FOV of the Front Camera, Centre - Forward Manipulator Position within the FOV of the Front Camera, Bottom - Minimum Clearance from DVL to the Seafloor.....	40
Figure 54: CAD model of T-slot Guide Rod on Linear Actuator	41
Figure 55: Left - Applied Forces on Servo housing, Right - Meshed Servo Housing	42
Figure 56: Servo Housing Static Stress Plot.....	42
Figure 57: Servo Housing Resultant Displacement Plot	42
Figure 58: Left - Applied Forces and Torque on Link 1, Right - Meshed Link 1	43
Figure 59: Link 1 Static Stress Plot.....	43
Figure 60: Link 1 Resultant Displacement Plot.....	44
Figure 61: Forces applied on Shaft.....	44
Figure 62: Shaft Static Stress Plot	44
Figure 63: Shaft Resultant Displacement Plot.....	45
Figure 64: Flow Simulation Results for Currents Flow of 1.5 m/s	46
Figure 65: CFD Results For Manipulator in Bottom-Facing Position	47
Figure 66: Pressure Simulation Results for Currents Flow of 1.5 m/s	47
Figure 67: Flow Simulation Results for Forward AUV Motion of 1.5 m/s	48
Figure 68: CFD Results For Manipulator in Keeping Position	48
Figure 69: Flow Simulation Results for Forward Actuation Motion in Back Currents of 1.5 m/s	49
Figure 70: CFD Results of Manipulator in a Forward Position	49
Figure 71: Left -Schematic Diagram of the Electrical Architecture for the Manipulator System, Right - Fabricated Manipulator Printed Circuit Board	50

Figure 72: Assembly of Servo Components.....	51
Figure 73: Assembly of Manipulator.....	51
Figure 74: Air Trials Results , Left – 45° Configuration, Right – 135° Configuration.....	52
Appendix 1 – Figure 75: Official Competition Rules for SAUVC 2016 and Robosub 2016 ..	57
Figure 76: Different grades of Coffee grains, with increasing coarseness from 1 to 4.....	63
Figure 77: Left - Fine Grain Coffee used to pick up a tweezer by the tip, Right - Coarse Grain Coffee used to pick up a tweezer by the tip.....	64
Figure 78: Left - Fine Grain Coffee used to pick up a tweezer by the flat side, Right - Mixture of Fine & Coarse Grain Coffee used to pick up a tweezer by the flat side	65
Figure 79: Left - Fine Grain Coffee used to pick up a pen by the cylindrical end, Centre - Coarse Grain Coffee used to pick up a pen by the cylindrical end, Right - Fine Grain Coffee used to pick up a pen from a bucket of water by the cylindrical end	65
Figure 80: Left - Fine Grain Coffee used to pick up a watch, Centre - Coarse Grain Coffee used to pick up a watch, Right - A mixture of Fine & Coarse Grain Coffee used to pick up a watch.....	65
Figure 81: Gripping of Various Objects in air trials; First row (from left) – K’nex structure, Optical Mouse, 25mm cylindrical light PVC pipe; Second Row (from left) – 32mm cylindrical PVC pipe, T-junction PVC pipe, 43mm cylindrical light PVC pipe; Third Row(from left) - 25mm cylindrical heavy PVC pipe, cuboid power bank, 43mm cylindrical heavy PVC pipe	72
Figure 82: HS-7950TH Servo Specifications (Servocity, 2016).....	73
Figure 83: CAD Model of Manipulator Arm	73
Figure 84: Gripping of Various Objects in air trials; First row (from left) – 25mm PVC Pipe, 43mm PVC Pipe, K’nex Structure, Second Row (from Left): U channel, Odd Geometric	

Structure, Square tube, Sphere ,Third Row (from left): 2 Pearl Weight, Screwdriver Head,	
Kick Board.....	76

List of Tables

Table 1: Characteristics, Advantages and Disadvantages of Manipulator Types (Kuttan, 2007) & (Circuitdigest.com, 2015).....	58
Table 2: Characteristics, Advantages and Disadvantages of Different Actuation Types.....	59
Table 3: Density of Common Granular Materials (Engineering toolbox, 2015).....	63
Table 4: Tabulation of Pre-Experiment Results of 5” Jamming Gripper	64
Table 5: Tabulation of Results of Gripping Various Weights using a 24” Jamming Gripper .	71
Table 6: Tabulation of Stepped-Up Servo HS-7950TH Characteristics	74

1. Introduction

1.1. Objectives

The objective of this project is to design and manufacture a robust, low cost manipulator to be used on board an Autonomous Underwater Vehicle (AUV). It will be customized to fit the Bumblebee AUV Version 3.0, an AUV designed and built by NUS students, where it will be integrated, operated and evaluated for its effectiveness.

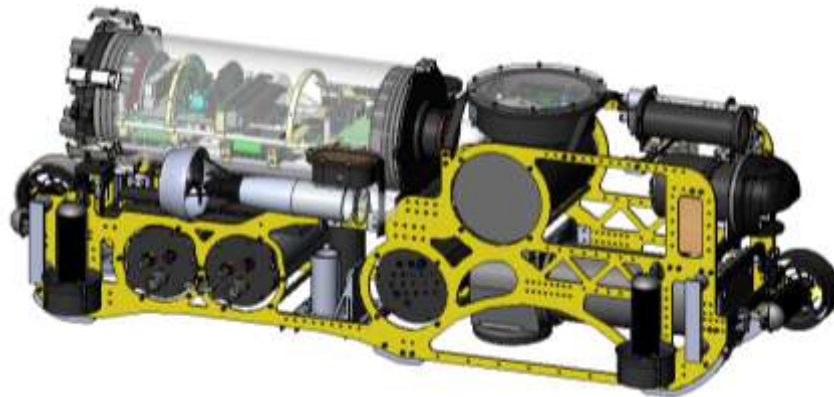


Figure 1: Bumblebee Autonomous Underwater Vehicle Version 3.0

1.2. Problem Statement

Underwater robotic arm technologies can either be very expensive or possess limited functionality (Cooney, 2006). Robotic arms with multiple degrees of freedom are typically designed for larger vehicles and higher depth rating, but are often expensive and heavy. An example is Schilling Robotics' Titan (Fig 2, left) which is dexterous and robust, but it is pricey and weighs up to 100 kg in air (FMC Technologies, 2015). In contrast, lower cost manipulators for instance, the three jawed Seabotix manipulators (Fig 2, right), (Seabotix, 2015), commonly have limited applications and capabilities, placing a greater dependence on vehicle maneuverability in order to achieve complex manipulator tasks.



Figure 2: Industry Underwater Manipulators; Left - Schilling Robotics TITAN 4 (FMC Technologies, 2015), Right- Seabotix Grabber on Remotely Operated Vehicle (Seabotix, 2015)

Furthermore, a motivation for this project is due to several limitations of the existing manipulator design on Bumblebee AUV Version 2.5:



Figure 3: 3D CAD of Manipulator Design for Bumblebee AUV Version 2.5

- 1) Low Versatility - Manipulator design is specific to item being grabbed, requiring change in shape of manipulator every year according to competition tasks.
- 2) Need for Accurate Positioning – When grabbing objects, there is a high reliance on proper positioning of the vehicle and grabber, resulting in a low success rate
- 3) Limited Capabilities - Grabber claws can only open and close. It is also installed at the bottom of the vehicle and is unable to do forward facing tasks.

- 4) Need for Redundancy: 2 sets of grabbers required for more stable grasp on larger objects, without which objects will dangle and sway.
- 5) Close Proximity required: When grabbing objects from the ground, vehicle has to go very closely to the object. This covers the bottom facing camera and prevents it from focusing on the object to pick up. Also, it causes a problem in the DVL sensor when minimum distance from the sensor to the sea floor $< 50\text{cm}$.
- 6) Prone to damage: 3-D printed Claws are easily broken off when vehicle is placed on the floor with closed grabbers because it protrudes out of vehicle.

1.3. Scope

The focus of this project is to design for functionality and system integration onto an existing AUV, which will be used to compete in the Singapore Autonomous Underwater Vehicle Challenge (SAUVC) organized by IEEE, and the 19th Annual International Robosub Competition organized by AUVSI Foundation. Following design, the manipulator arm will be fabricated, and in-depth experimentation will be performed to test out the effectiveness of the design. Besides being reliable, it is essential that the system stays within the design constraints imposed by competition rules and also within the requirements of the sensors on the AUV.

1.3.1. Design Constraints

For proper integration of the manipulator to the main vehicle, the manipulator must adhere to the following characteristics:

- 1) Compact Size & Lightweight

The AUV must comply with competition specifications (Appendix 1) – which impose an upper limit of 50kg and 140x91x91(cm) in dimensions, otherwise there will be points

deduction or disqualification from the competition. Hence, an arm that is light and able to be folded for keeping is advantageous in reducing the overall weight and length of the AUV. Moreover, a compact arm will encounter less drag force which improves manipulation performance.

2) Positioning

The available space on the AUV to mount the manipulator is the area marked in red (Fig 4).

The form and type of arm that can be used is limited by the occupancy of various sensors and thrusters which the arm needs to steer clear of, as shown in Figure 5.

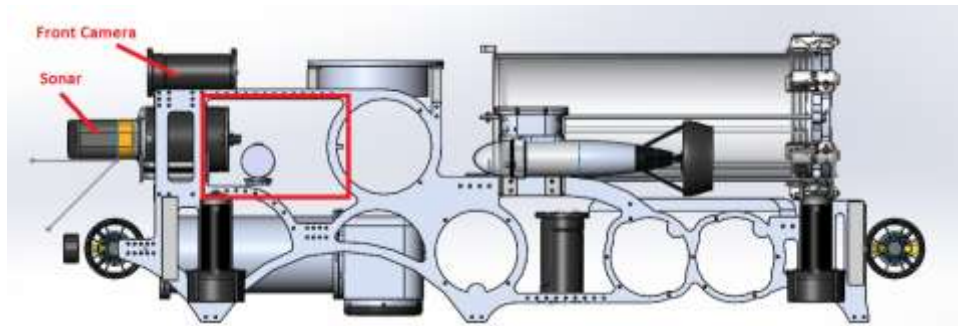


Figure 4: CAD of Available Mounting Space for Manipulator on Bumblebee AUV marked by red box

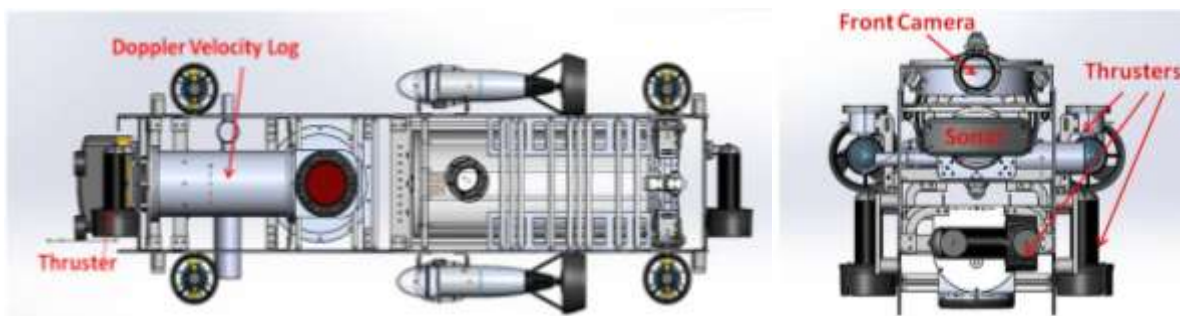


Figure 5: Left - Lack of available space at the Bottom due to the Doppler Velocity Log Sensor, Right - Lack of available space at the Front due to occupancy by the Front Camera, Sonar, and Yaw Thrusters

3) Pressurised gas

The rules (Appendix 1) capped the compressed gas pressure to be 6 bars, and the current portable compressed air tank on the vehicle has a capacity of 13 cu in, so the usage of any pneumatic components must keep within these specified limits.

4) Maximum power voltage

The rules (Appendix 1) capped the maximum power voltage to be 24V DC, so the usage of any electrical components e.g. motors and regulators should keep within these requirements.

1.3.2. Competition Manipulator Tasks

The manipulation tasks varies across the years, and they included - turning a steering wheel, lifting and sliding a handle off a board, and picking and placing of different objects such as PVC pipe structures or K'nex structure etc (Fig 6).

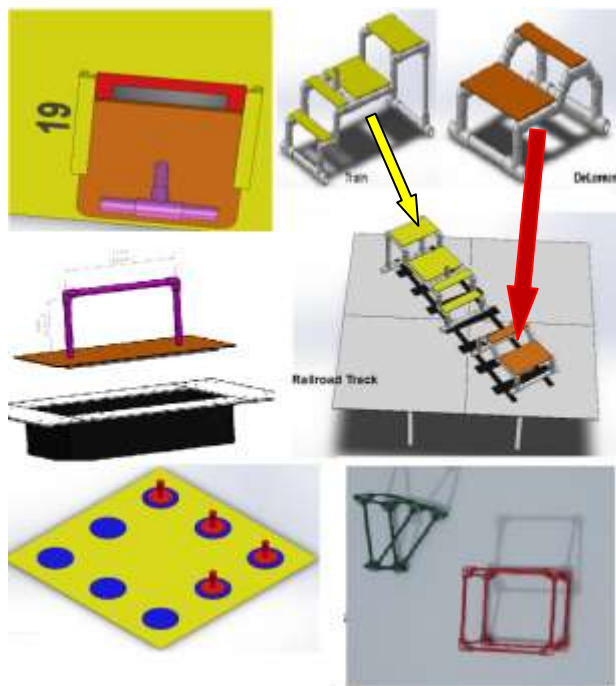


Figure 6: Examples of Manipulation Tasks at the AUV Competitions

2. Literature Survey

Literature research was carried out to generate design ideas on how the manipulator and gripper should be developed.

2.1. Manipulator Arm Types

The body structure of a manipulator determines the functions, reach, orientation and the overall workspace. Also, the joint types used to connect different members of the manipulator determine the overall degrees of freedom of the manipulator in motion (Brighthub Engineering, 2015).

There are many types of industrial manipulators and the type is selected depending on its pros and cons as well as the application requirements. Table 1 (Appendix 2) displays the common types of arms used in the industry into 5 categories - Cartesian, Cylindrical, Polar, SCARA and PUMA. The study of the various types influenced the design process of the manipulator arm which will be covered in Section 4.

2.2. End-effector Types

The end-effector, commonly known as a gripper, is crucial because it is the mechanical interface between the robot and the work environment (D.T. Pham and S.H. Yeo, 1988). It facilitates temporary contact with the manipulated object, ensuring its position and orientation during transport and specific activities. There are many different types of gripper mechanisms, which Nair (2009) classifies into 3 categories:

- 1) Mechanical Finger Grippers (Sub-classification is based on actuation method)
- 2) Vacuum and Magnetic Grippers (Sub-classification is based on type of the force-exerting elements)

3) Universal Grippers (Sub-classification is inflatable fingers, soft fingers & three fingered grippers)

In terms of actuation, there are generally five types- Pneumatic, Hydraulic, DC Motors, AC Motors and Vacuum actuation. Table 2 (Appendix 3) categorises the various types of actuations, their characteristics and applications, as well as the pros and cons associated with their usage. Additionally, research was carried out on a unconventional technique which combines pneumatic and vacuum actuation, known as the Universal Jamming Gripper technique.

2.2.1. Universal Jamming gripper technique using granular material

The Universal Jamming Gripper consists of a mass of granular material encased in non-porous elastic membrane (Brown et al., 2010). Through a combination of positive and negative pressure, the gripper can rapidly grip and release a wide range of objects. In Fig 7, the gripper passively conforms to the shape of a target object, and when a negative pressure (vacuum) is applied, the granular materials become stiff, achieving a rigid grip. Positive pressure is then utilized to reverse this transition—releasing the object and returning to a deformable state.



Figure 7: Empire Robotics' VERSABALL Gripper Conforming to Shape and Lifting Objects; Left - Hammer, Right - Brick, (Empire Robotics, 2016)

Granular Behaviour and Properties

Granular material exhibit both fluid-like and solid-like states (Fig 8). Naturally they exist in fluid-like state, where excess interstitial fluid (typically air) is enclosed with the loosely-packed particles and they flow freely when subjected to external forces. Hence, when pressed on an object, the particles surrounds and takes the shape of the object it is grasping.

Meanwhile when a vacuum is created to remove the interstitial fluid, the flexible membrane in an attempt to equalize the pressure constricts the particles, causing them to shift and fill up the voids left behind by the evacuated fluid, e.g. Air. Thus, the packing factor and the contact networks between the particles increases (Fig 9), and they become solid-like (Mozeika, 2016). This is known as jamming, where granular materials exhibit a yield stress such that forces can be distributed through groups of particles and as a whole it can function as a compliant or stiff material (Follmer, Leithinger, Olwal, Cheng, & Ishii, 2012).

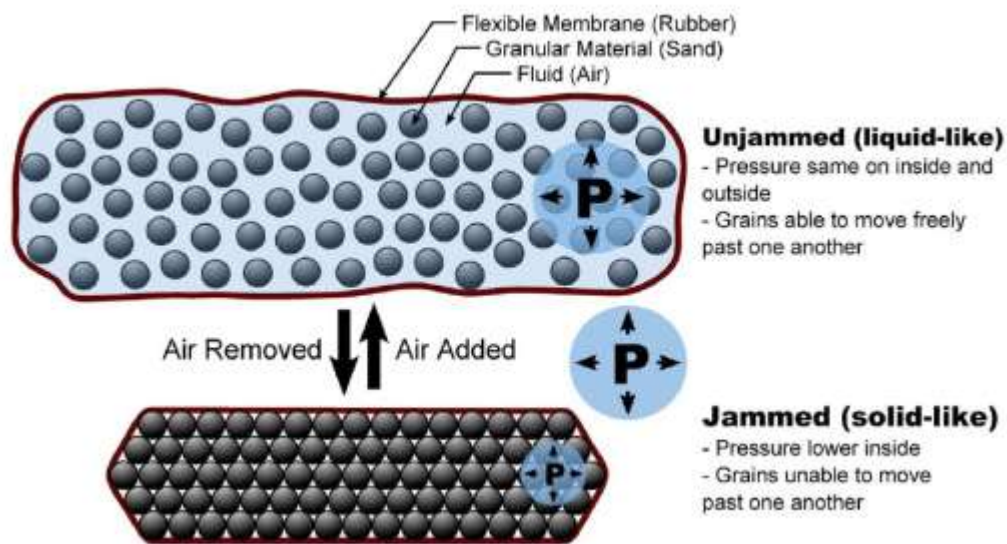


Figure 8: Granular interaction in unjammed (fluid-like) and jammed (solid-like) states (Mozeika, 2015)

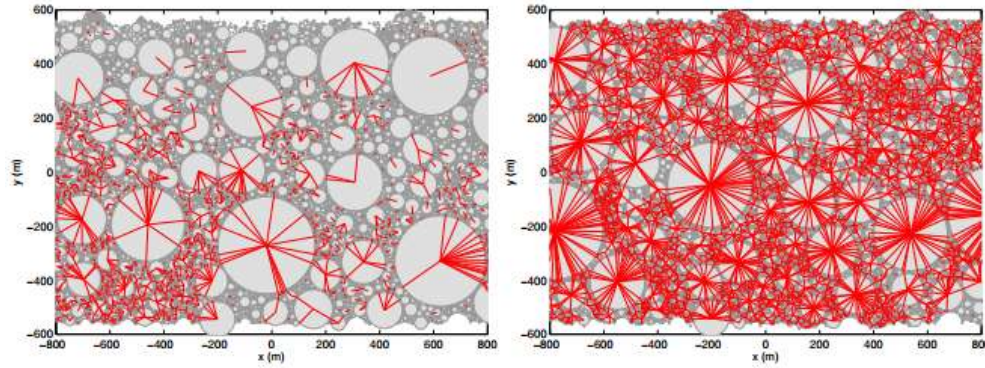


Figure 9: Contact Networks in the Modeled System; Left - Unjammed state (Packing = 89%) , Right - Jammed state (Packing = 90.5%) state. For each grain, i, a line is drawn from its center to the neighboring grain (Herman, 2013)

Vacuum generator

Evacuation of air can be achieved by the vacuum generator, a lightweight and compact device that generates a vacuum using the Venturi principle, where the motion of a moving fluid (motive fluid such as compressed air) is used to transport away another fluid, creating suction (Fig 10, left). As the tube narrows at the diffuser throat, the velocity of the fluid increases, Bernoulli's principle (Fig 10, right) states that there will be a resulting proportionate decrease in pressure in order to maintain the same total mechanical energy (= Potential Energy + Kinetic Energy + Pressure Head). As air moves from a location of high pressure to low pressure, the low pressure region in the diffuser causes air to rush in through the suction port, generating a vacuum. The commonly used vacuum units is Torrs (mmHg).

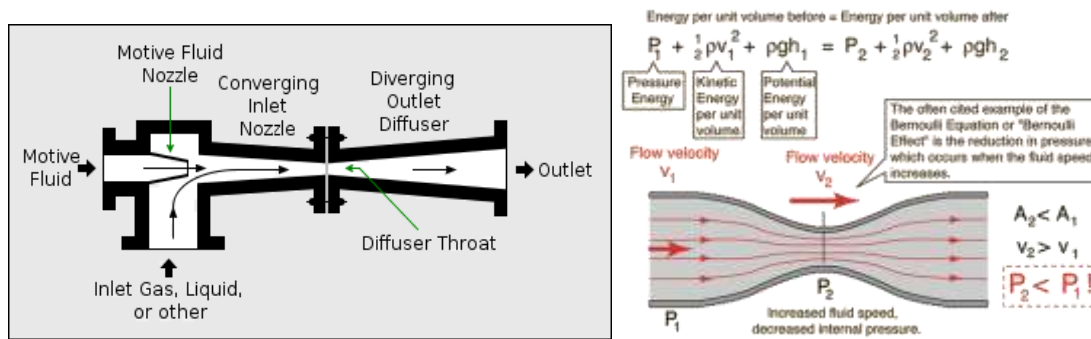


Figure 10: Left - Features of the Vacuum generator, Right - Bernoulli's Equation (Hyperphysics, 2015)

Gripping Mechanism

This gripper leverages three possible gripping modes for operation as can be seen from Fig 11:

1) static friction from surface contact; 2) geometric constraints from capture of the object by interlocking; and 3) vacuum suction when an airtight seal is achieved on a portion of the object's surface. The friction force results from the slight ($<0.5\%$) volume contraction of the membrane that occurs during evacuation, which, in turn, causes a pinch force to develop, normal to the point of contact. Slip can be prevented either by friction from contact pressure or by exploiting geometric constraints, for example by wrapping around protrusions. By achieving one or more of these three gripping modes, the jamming gripper can grip many different objects with diverse shapes, weights, and fragility, including objects that are traditionally challenging for other universal grippers (Amend et. al., 2012).

The key parameter that determines the gripping strength is the holding force F_h . A set of equations derived by Brown et. al. (2010) through experimentation on test spheres of varying radius R can be used to describe contributions to holding force F_h for the three gripping modes (Appendix 4). In summary, Brown's results demonstrated that the holding force F_h is mainly dependent on friction and suction mechanisms, which builds up when the contracting membrane compresses against the object to be gripped; meanwhile contributions from geometric interlocking depends on the extent of interlocking and can involve the full stress-strain curve. Other secondary parameters that are directly proportional to the gripping strength are: the properties of the granular material in jammed state (i.e. the size, shape and surface roughness which affects granular strength and rigidity), the confining pressure induced by the vacuum, hardness of the objects being grabbed, surface contact angle of the gripper-object interface and membrane elasticity (Brown et. al., 2010).

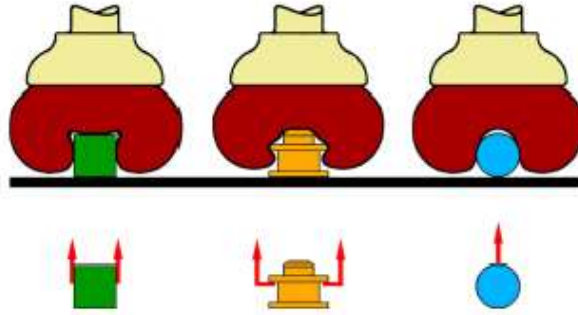


Figure 11: Three gripping modes of Jamming Grippers, Left -Static friction from surface contact, Centre - Geometric constraints from interlocking, Right - Vacuum suction from airtight seal, (Amend et al, 2012)

Granular jamming gripping technique as the End-effector Choice

The jamming gripper is advantageous as it can grab a wide variety of arbitrarily shaped objects. Also, it eliminates the computational complexities presented by active grippers, notably the multi-fingered arms within dependently actuated joints. Moreover, the gripper possesses high reliability, error tolerance, and placement accuracy (Amend, Brown, Rodenberg, Jaeger, & Lipson, 2012). Given the competition constraints and task requirements, these factors make it suitable for application on the Bumblebee AUV.

In this project, its potential usage in the underwater realm will be explored, where the increasing pressure with depth may aid in enhancing the gripping force. Also, experimentation will be conducted on various types of objects before conducting evaluation on the gripper performance, as previous test experiments conducted by researchers made use of spheres as target objects which may not be sufficient. Additionally, design aspects will be improved to optimize the gripping capabilities. Hence, this universal jamming technique will be adapted and the design modified to suit underwater usage and installation onto the Bumblebee AUV.

3. Mechanical Design of End-effector

To enable robust gripping capabilities, recommendations from literature research were used to identify the most suitable components and materials required to build the jamming manipulator, and datasheets of these components were thoroughly read before procurement.

3.1. Components of the Jamming Gripper

The choice of granular material, Coffee powder, was due to its lowest density amongst common granular materials (Appendix 5). Several grades of coffee powder ranging in coarseness were selected as granular material to be pre-tested (in section 3.2), to identify the ideal granular size for gripping. This is because Brown (2010) suggested that small grain sizes is advantageous as it increases the degree of conformation, but not too small as the gas permeability of a powder scales with the square of the grain diameter; hence, decreasing grain diameter increases the pumping time required to reach a strongly jammed state.

Meanwhile, considerations for the membrane include flexibility for better conformation, impermeability to allow for pressure build up during jamming, and a coefficient of friction $\mu \approx 1$ for friction or suction to work at small contact angles. Hence, a standard size 5" Natural Rubber balloon was used as the elastic membrane.

3.2. Pre-experiment

Initially, a simple experiment was carried out to test the feasibility of the jamming technique and to gain an understanding of the control variables and how they affect the experiment. To create a vacuum required for granular jamming, a syringe was used (Fig 12, left). However, the sealing using a tape was ineffective and a near-vacuum condition cannot be created, resulting in the inability to harden the grains. The syringe was subsequently replaced by a

soap dispenser of a diameter slightly larger than balloon mouth to create an effective seal (Fig 12, right), and air can be constantly expelled out thus generating near-vacuum conditions.



Figure 12: Jamming Gripper Mini Experimental Set-up

Objects of varying shape and weight were lifted, and tested in air and in a small bucket of water (water column height = 100 mm, external pressure ~ 0.01 bar). Trials were performed on fine grains, coarse grains and a mixture of both grains (amount of each weighs $\frac{1}{2}$ of the total weight). Trials were repeated 3 times, and the more common result taken to be recorded in Table 4 (Appendix 6).

Several observations are made from the experiment:

- 1) High success rate of picking up objects smaller than the membrane diameter and objects wrapped around $>75\%$ by the membrane (3 out of 4 object faces in contact with the membrane).
- 2) Possibility for the grains to pick up objects exceeding its weight by 8 times
- 3) The experiments in water tend to fail more than on air because of slip due to reduced friction between object and walls of the membrane
- 4) For fine grain material, it is relatively more successful in picking up objects with complex geometries.

This is supported by Herman (2013), who asserted that fine particles act as “fillers” in the empty spaces between coarser grain particles, which flows more easily to fill up the voids created by the object geometry, resulting in a greater conformation to the object shape and a more secure grip. This is observed when comparing Fig 13 left and centre images. Also, as seen in Fig 13 (right), combining both fine and coarse grains in the membrane gave a similar outcome as the sole use of fine grains.



Figure 13: Left - Fine Grain Coffee enables relatively higher object conformation, Centre – Coarse coffee enables relatively lower object conformation, Right – Fine & Coarse Grain Mix enables relatively higher object conformation

- 5) For coarse grain materials, it reduces slipping tendencies and is more able to pick up objects with less contact points, i.e. flatter objects.

As seen from Fig 14, after the removal of the objects, the membrane remains deeply etched by the object for coarse grain materials (centre) as compared to the fine grains (left). This is explained by the higher rigidity of coarse particles, ie. resistance for grains to flow past each other in vacuum state, thus retaining its form and increasing gripping strength on the object. Herman (2013) supports this from his statement that it is the coarse particles which forms the “stable skeleton of the global and force network”. Moreover, Xu and Ching (2010) stated in

support that coarse particles are easier than fine particles to *jam*. Combining both fine and coarse grains also resulted in a similar outcome from solely using coarse grains (Fig 14, right).

- 6) The combination of both fine and coarse grain materials encompasses the merits of each individual grain type.



Figure 14: Left – Fine Grain Coffee leaving relatively Less Defined Imprint on membrane, Centre - Coarse Grain Coffee leaving relatively More Defined Imprint on membrane, Right – Fine & Coarse Grain Mix leaving relatively More Defined Imprint on membrane

Based on these observations, it is deduced that a mix of both fine and coarse grains should be used in the actual prototype, and the balloon membrane has to be sufficiently big to grip the structures used in the competition. The standard-size 5” balloon was far too small for grabbing most objects and so it was replaced by a 24” latex balloon. The design of the gripper segment was affected by these observations and it will be elaborated upon in the subsequent section.

3.3. End-effector Design

3.3.1. End-effector Design 1

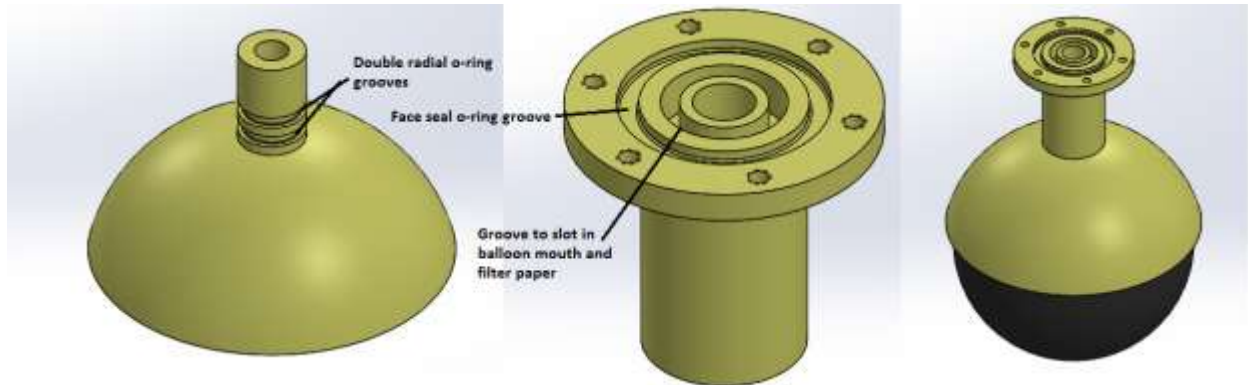


Figure 15: Gripper Collar assembly consisting of cup and throat

The gripper collar assembly shown in Figure 15 will be made of T6-6061 Aluminium, a light and relatively corrosion-resistant material, and it is designed as an assembly of two separate parts – the cup and throat, to simplify the machining process. To seal the collar properly and prevent water entry into the balloon, there are 2 radial o-ring grooves on the cup, which will be compressed when the throat is plugged onto it. The throat also contains an outer o-ring groove meant for face sealing, where the o-ring will be compressed by a lid using 6 bolts. The inner groove on the throat is designed to be deep and wide to slot in both the balloon and a filter paper which prevents the suction of grains into the vacuum pump.

A 3D printed prototype was constructed for testing its effectiveness, and it was observed that a rounded deep cup (Fig 16, left) was relatively inefficient for gripping objects of larger diameters or lengths in comparison to a shallower but wider cup (Fig 16, right). This is because enclosing larger objects within the grasp was inhibited by the rim of the deep cup, and in the process many grains were trapped against the cup walls and unutilized, rather than

being made to flow around the object for gripping. Meanwhile, the shallow cup manages to shape the grains to better surround the object for a more efficient gripping.



Figure 16: 3-D printed prototypes of Gripping cups - Deep cup versus Shallow wide cup



Figure 17: Assembly of End-effector

A series of mini tests were performed on the actual sized prototype, a 24” balloon filled with a mixture of fine and coarse grains. To achieve a vacuum for the jamming of grains, a vacuum generator VADMI 45-LS-P sponsored by Festo (Appendix 7) was chosen for its high vacuum percentage of 85% or 115 Torrs, modularity and air saving circuit. The vacuum generator was connected to a power source and a gas compressor, generating a suction effect in the balloon. This was demonstrated on several objects as shown in Fig 18 and gripping was successful.



Figure 18: Left - Vacuum Pump is connected to the 24" gripper via Custom-made adaptor, Centre - Jamming Gripper is successful in picking up the oval metal structure, Right - Jamming Gripper is successful in picking up the K'nex

Being electrically activated, the plan for the vacuum generator is to be located in the pneumatic hull of the AUV, which currently houses pneumatic components such as the solenoid valves, manifold rail and pneumatic fittings. The pneumatic hull was chosen to keep it waterproof and enable it to be conveniently connected to the solenoid valves, which control the power and air supplied to the pump. Externally, the pneumatics hull comes in three parts: the front cap; the hull body; and the end cap which holds up the solenoids using a mount for easy disassembly during maintenance (Fig 19).

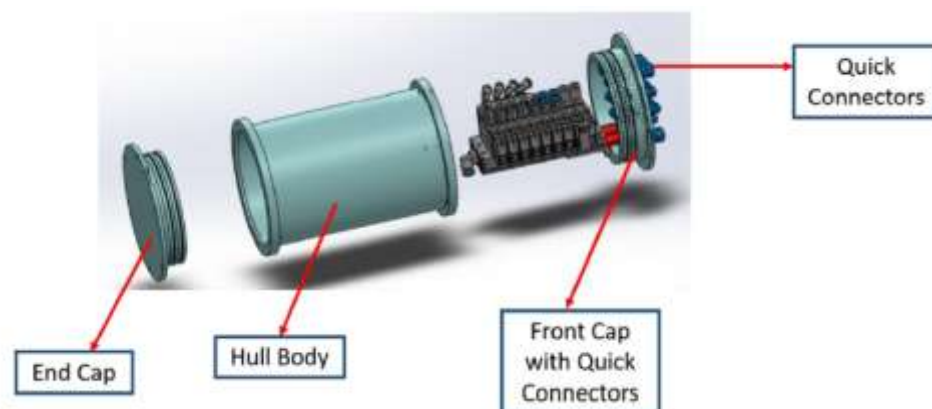


Figure 19: Partially Exploded CAD View of Pneumatic Housing

As the pneumatic hull was fabricated earlier before the conception of this project, there was limited space inside for the vacuum generator. Hence, a uniquely shaped 3D printed part shown in Fig 20 (left) was designed to mount the vacuum generator in an inclined position to fit into the existing design of the pneumatic hull (Fig 20b).

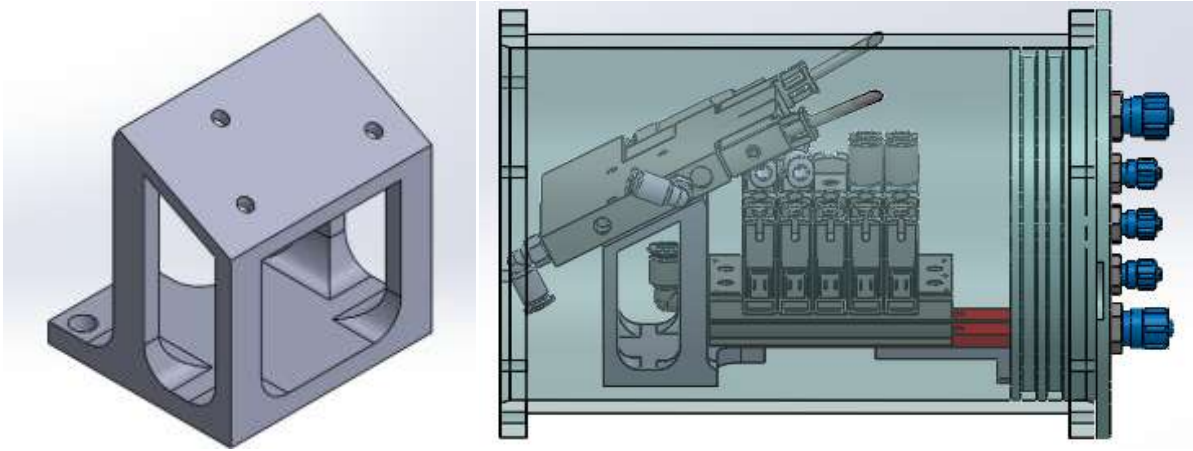


Figure 20: Left - Isometric CAD View of the Vacuum Generator Mount, Right - CAD Assembly of the Vacuum Generator inside the Pneumatic Hull

3.3.2. End-effector Design 2

Upon submersion of the prototype in water, the water entry points were better understood (Fig 21, right) -water enters from underneath the cup and through the flange. Moreover, to cut down costs from having to fabricate separate pieces, the gripper throat and cup components (Fig 17) were combined to form a single piece design. The enhanced gripper design as shown and labeled in Fig 21 (left) has a face seal at the top and an internal radial o-ring seal, compressed respectively by the gripping support and aluminium cap for sealing off water entry. The o-ring groove dimensions are designed according to recommendations by Parker Hannifin Corporation (Appendix 9) and the o-rings selected are of standard size.

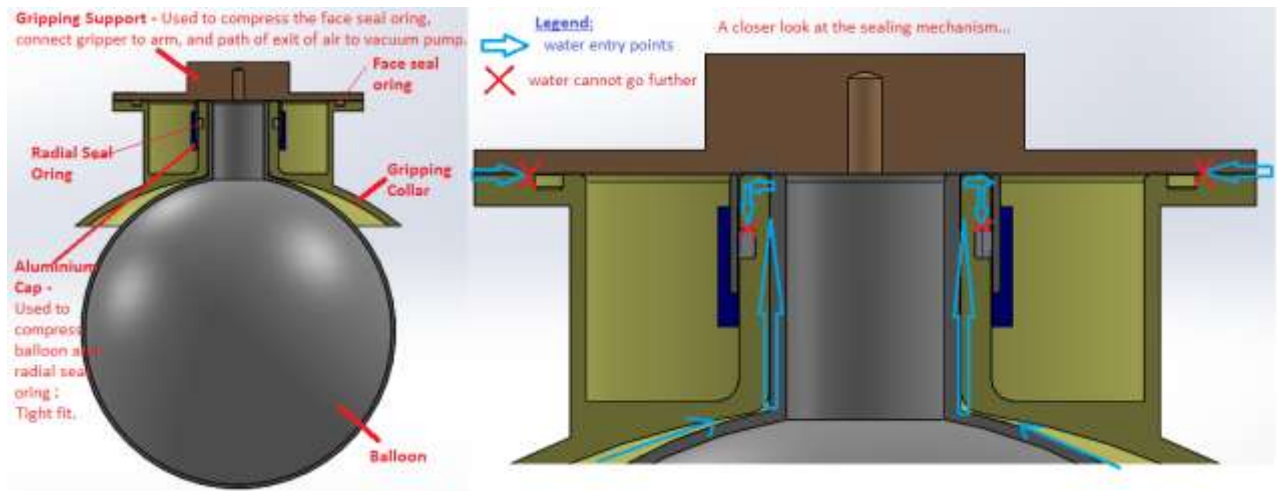


Figure 21: Left - Cross-sectional CAD of End-effector Design 2; Right - Water Entry Points of End-effector

Meanwhile, the lid meant for compressing the face seal o-ring (gripping support) was designed as shown in Fig 22, with an L-shape hole for air flow away from the membrane to the vacuum generator during suction via pneumatic tubings, joined by a Festo push-fit connector, QSML-M5-6 (Appendix 8). It also contains threads to be bolted to the main arm (consisting of a threaded linear piston) and guide rods for distributed support of gripper weight, as will be elaborated later in Section 4 – Mechanical Design of the Manipulator Arm.

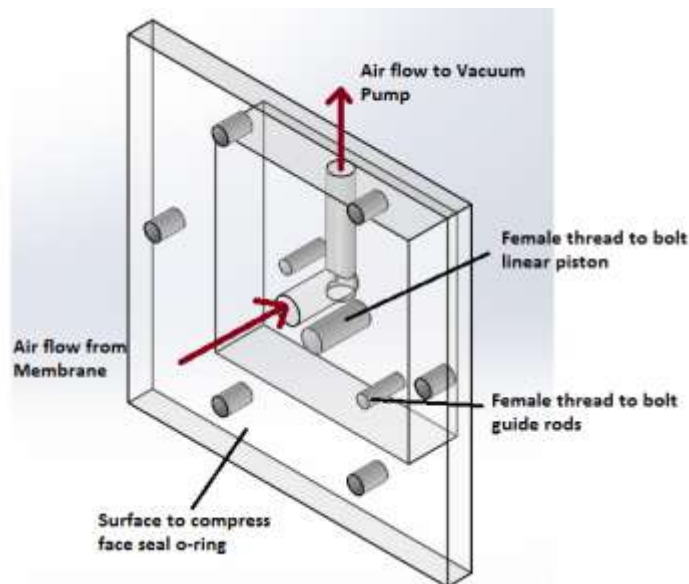


Figure 22: CAD Diagram of Gripper Lid Support



Figure 23: Left - 3-D Printed ABS Prototype of Design 2 End-Effector, Right - End-effector Assembly comprising 3D printed Gripping Collar, Latex Balloon, Coffee Powder and Filter Paper

A prototype of Design 2 was 3-D printed using ABS plastic filament for a smooth glossy finish and then assembled (Fig 23). The trial in air was successful in which a balloon filled with 80g of coffee powder managed to pick up a PVC structure of at least 5 times its weight, as shown in Fig 24. The setup failed during water trials because water went into the balloon, arguably because of the unsuitability of 3D printed parts where warping during the printing process resulted in non-uniformity and some porosity for water to flow through.



Figure 24: Left - End-effector lifting up a PVC pipe structure of weight 475g, Right - Weight of PVC pipe structure

3.4. Fabrication and Testing

With successful trial grabs by the jamming gripper in air, the design was proceeded to be fabricated in Al T6-6061, a light metal which is easy to machine, has high strength and has high corrosion-resistance. The fabricated collar and lid are shown in Fig 25, with the lid corners (Fig 22) filleted to remove excess material and reduce overall weight of the gripper.



Figure 25: Left - Gripper Collar, Right - Gripper Lid

3.4.1. Testing in Air

The objective of this trial is to test the reliability of gripping various objects, and identify any limitations to improve gripping performance. The test setup consists of a 24" balloon 60%-filled with coarse and fine mix of coffee (105g), a vacuum generator, a power supply and an air compressor. Objects of diverse shapes, weight and dimensions, including competition-used objects i.e. PVC pipes were each picked up 10 times and the success rate recorded in Table 5 (Appendix 10). Each trial involved lifting the object and subjecting the gripper to a vigorous sideways swaying motion to determine if the grip exerted on the object is sufficiently firm.



Figure 26: Setup of Jamming Gripper Experiment in Air

The results (Appendix 10) in general show that gripping reliability increases with decreasing object weights and dimensions. From the differing success rates, the following characteristics were observed about the gripper:

- 1) 100% success rate: Gripper contacts the ground and is pressed flat during gripping; at least $\frac{3}{4}$ of the object surface is wrapped by the membrane (Fig 27).



Figure 27: 100% gripping success case, Left – Gripper contacts ground (Flat underneath), Right - $\frac{3}{4}$ or more wrap-around Diameter

- 2) 80% success rate: Less than $\frac{1}{2}$ of the object total surface area is wrapped by the membrane; Object engages in geometric interlocking with membrane due to complexity of object geometries (Fig 28).



Figure 28: 80% Gripping Success Case from Geometric Interlocking with $\frac{1}{2}$ or less wrap-around Diameter

- 3) 20% success rate: Gripper does not contact the ground; membrane wraps $\frac{1}{2}$ or less of the object surface area (Fig 28).



Figure 29: 20% gripping success case, Left– Gripper does not contact ground (Round underneath), Right - $\frac{1}{2}$ or less wrap-around Diameter

From this experiment, it is deduced that it is highly difficult to grasp objects with smooth, uniformly curved geometries (PVC straight pipe) rather than geometrically complex objects (PVC T-junction). The reason is that friction is very low for these smooth objects, resulting in only the suction gripping mode being utilized for the former case, while suction plus geometric interlocking modes for latter case. For gripping such objects, it is therefore essential to ensure a sufficiently large granular membrane to surround at least $\frac{3}{4}$ of the object to simulate a geometric locking which will enhance reliability. This criterion can be simply fulfilled by observing that the bottom of the gripper is compressed flat during object gripping.

3.4.2. Testing in Water

The objective of this experiment was to test the waterproof design of the gripper, its ability to grip objects in underwater conditions and the gripping technique to be used. A similar experimental setup as in Section 4.1 was put up at Queenstown Swimming Complex's diving pool, with the vacuum generator powered by a 24V 3000mAh battery. The gripper turned solid hard within depth of 2m (0.2 bar pressure) without the need to operate the vacuum

generator. To pick up objects, positive pressure had to be input into the gripper to inflate it to surround the object, before applying a negative vacuum for suction. The successful outcome of gripping of 25mm pipe when using the 24" balloon as before was low. It was observed to be more challenging than in air because of the drag force of the water, greatly reduced friction at the gripper-object interface and the floatability of the low density grains which reduced conformability around the objects.



Figure 30: Experimental Setup for testing Jamming Gripper in Water

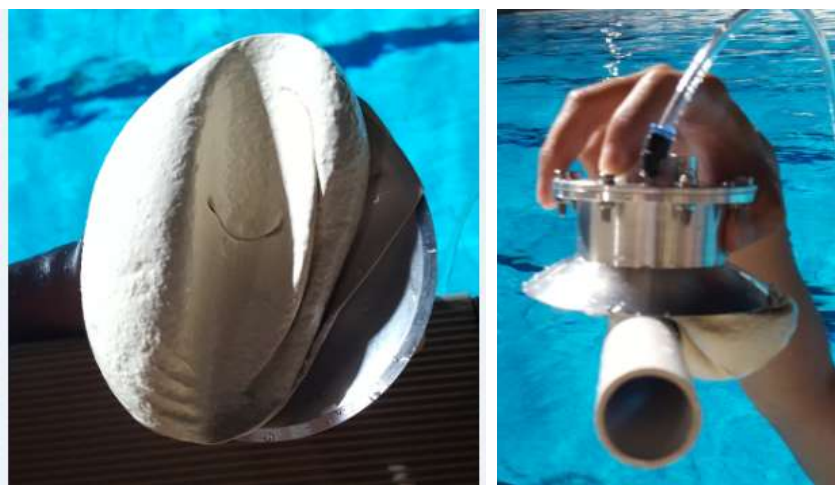


Figure 31: Irregular Object Conformability of Jamming Gripper of a smaller, less packed membrane

To achieve a higher reliability of gripping in water, the 60%-filled 24” membrane was replaced with an 80%-filled 36” membrane (Fig 32) to increase the likelihood of grains surrounding the object and establishing a firmer grip. This time, gripping was successful during all the trials. The downside was the increased amount in air required, as it took 14 seconds to inflate and deflate the larger membrane for grabbing.

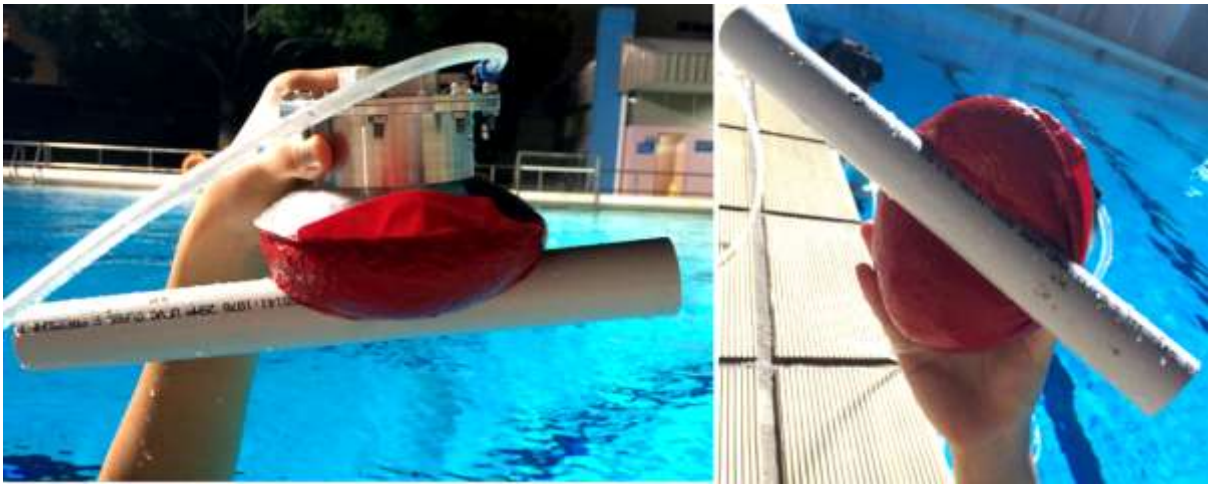


Figure 32: Successful Gripping using Jamming Gripper of larger, more highly packed membrane

4. Mechanical Design of Manipulator Arm

The design of the manipulator arm, the body structure which determines the functions, reach, orientation and the overall workspace, was based on an iterative process. This section talks about the generation of designs based on the AUV requirements and constraints and the recognition of the limitations which led to the generation of an improved design.

4.1. Design 1

The initial idea of the manipulator is a 3 DOF arm consisting of three rotational joints actuated by waterproof servos (Fig 33). The arm has a fairly large reachable workspace as it can position itself in all 3 dimensions and also rotate about 2 axes. This gives the arm relatively

high positional accuracy and a better reach to the objects, reducing the need to reposition the entire vehicle to access the object.

There are three links that make up the backbone of the arm – Link 1, Link 2, and Link 3.

Firstly, Link 1 which supports the bulk of the manipulator weight has a high tendency to fail, and material is removed in the form of triangular cutouts so as to create a truss structure to retain the structural stability of the linkage. Meanwhile, Link 1 Support connects the manipulator to the AUV frame and supports a waterproof servo which actuates Link 1. For Link 1 Support to withstand the entire manipulator weight, its structural channel is made to be an Aluminium U-bracket which is strong and lightweight (Sapagroup.com, 2016). Also, the U-bracket width is sized such that the arm will not collide with the side thruster during motion. Next, the unique design of Link 2 allows for 2 axis of rotary motion. Finally, Link3, which does not need to support a heavy weight compared to Link1, has more material removed so as to reduce the overall weight of the manipulator. The adjacent links are connected to each other via a cam follower (Fig 34), which combines a standard bearing on one end and a bolt on the other. Also, a flanged shaft hub (Fig 35) is selected to attach a waterproof servo to each link and rotates it with respect with the following link.

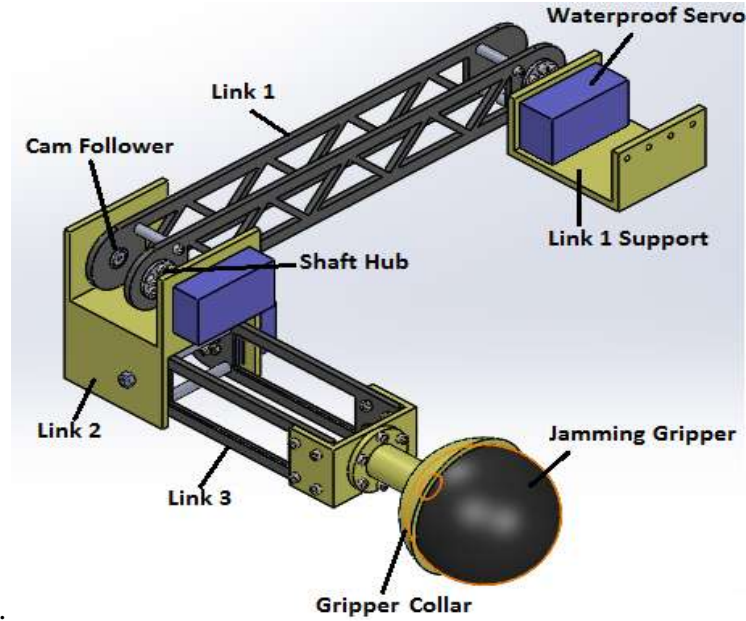


Figure 33: CAD model of Manipulator Design in a Keeping Position

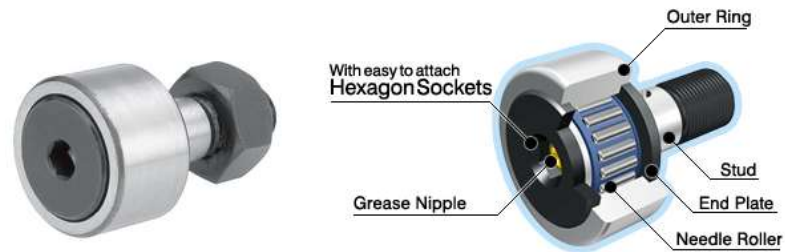


Figure 34: Left - CFFAP6-16 Cam Follower (Misumi, 2016), Right - Cross-section of a cam follower (Ikont.co.jp, 2016)



Figure 35: Servocity Flanged shaft hub (Servocity.com, 2016)

The arm is designed in this manner to achieve several important configurations of the arm (Fig 36 and 37) which have the following necessary functions:

- 1) Keeping: Reduction of drag and safe storage of manipulator during AUV motion
- 2) Forward: Grab or slide objects in front of AUV

- 3) Scooping: Grab or scoop up objects in front of AUV
- 4) Picking: Pick and place objects below AUV
- 5) Downward: Pick and place objects below AUV

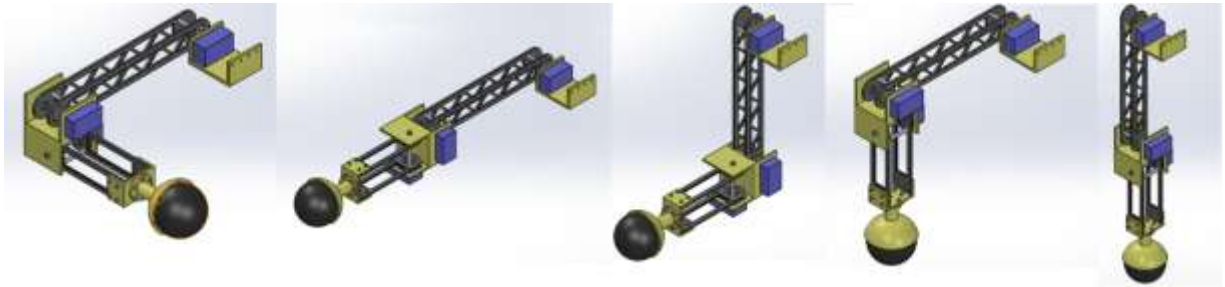


Figure 36: Manipulator Configurations - Keeping, Forward, Scooping, Picking, Downward positions

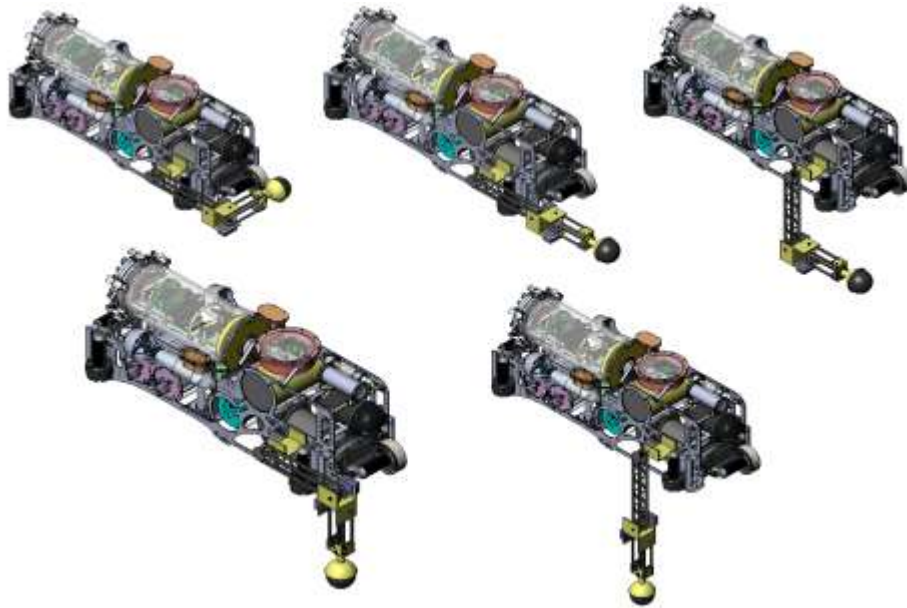


Figure 37: Manipulator Configurations on AUV- Keeping, Forward, Scooping, Picking, Downward

4.1.1. Limitations of Design 1

The difficulties of building a new component on an existing AUV design shows up in the limitations, which were discovered up on discussions with the team and further research, leading to the development of Design 2.

- 1) Keeping configuration creates several problems – Blocking the sonar and increasing the overall length of the AUV which leads to disqualification based on the competition rules.
- 2) Waterproof servos in the market are best rated IP67 which can only withstand water immersion of 1m for approximately one hour, and thus are not feasible for this application where it will be submerged for a long time period in deep waters beyond 5m.
- 3) Creating additional waterproof housings for three servos in total was impractical as it will increase the overall weight of the arm, requiring too high a torque to actuate the arm.

4.2. Design 2

Design 2 (Fig 38) features a less complex version that addresses the previous limitations and still meets the AUV requirements and functionality. The arm is lighter, dimensioned from standard parts, and actuated by pneumatic actuators rather than servos. It is a 2 DOF system consisting of a translational joint actuated by a Festo linear piston (ADN-12-250-APA), and a prismatic joint actuated by a Festo semi-rotary flanged actuator (DSM-12-270-P-FW-A-B) selected based on torque requirements (Appendix 11).

Basically, the arm has three configurations (Fig 39) – Forward, Downward and Keeping, to achieve the essential operations of Front-facing tasks, Bottom grabbing tasks and storing it in a safe location during AUV motion. Link 1 is a standard Aluminium U-channel which carries the rotary actuator which rotates to achieve these three essential positions. Meanwhile, Link 2 is a standard square tube supporting a Festo linear actuator via 3-D printed support mounts. Next, the linear actuator is connected to the gripper via the threaded piston, with the addition

of threaded guide rods which help to share the weight of the gripper and prevent unwanted free rotation of the gripper with respect to the arm.

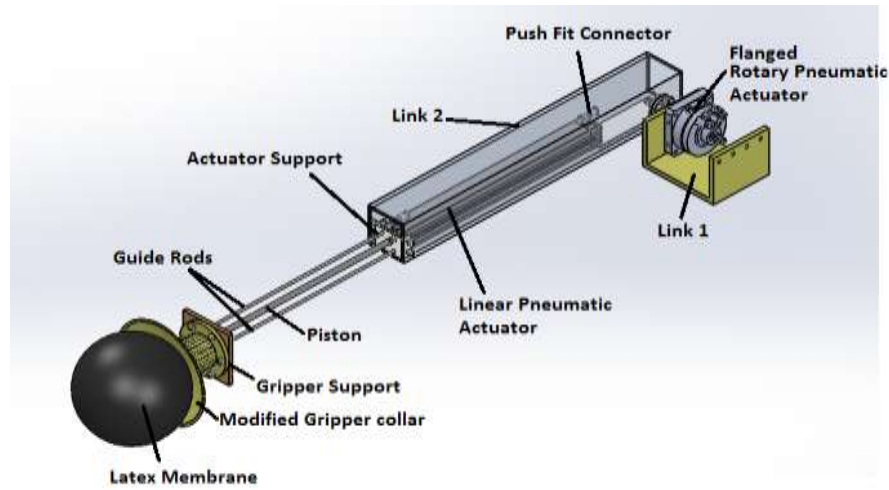


Figure 38: CAD model of Manipulator Design in a Forward Extend Position



Figure 39: Manipulator Configurations on AUV- Forward, Downward and Keeping Positions

4.2.1. Enhancements to Design 2

Design 2 was enhanced subsequently due to identification of several flaws, such as the inability to achieve the 3 required positions with just one semi-rotary pneumatic actuator. The working principle of the rotary actuator (Fig 40) is such that depending on the flow direction of the compressed air, a pointer swings between 2 extreme ends, and is stopped by a shock absorber on each end. The pointer is connected to the arm and so the location of the two shock absorbers determines the position of the arm. Hence, 2 semi-rotary pneumatic rotary actuators are needed since each rotary actuator can only achieve 2 arm positions.



Figure 40: Working Principle of Festo Semi-Rotary Pneumatic Actuator (Festo, 2015)

Furthermore, to decrease the overall manipulator weight while maintaining structural integrity, the top surface is removed from the originally square-tubed Link 2, and triangular cutouts further removed giving it a stable truss structure. The enhanced design, Design 2.5, is shown below in Fig 41 and the possible configurations of the arm in Fig 42.

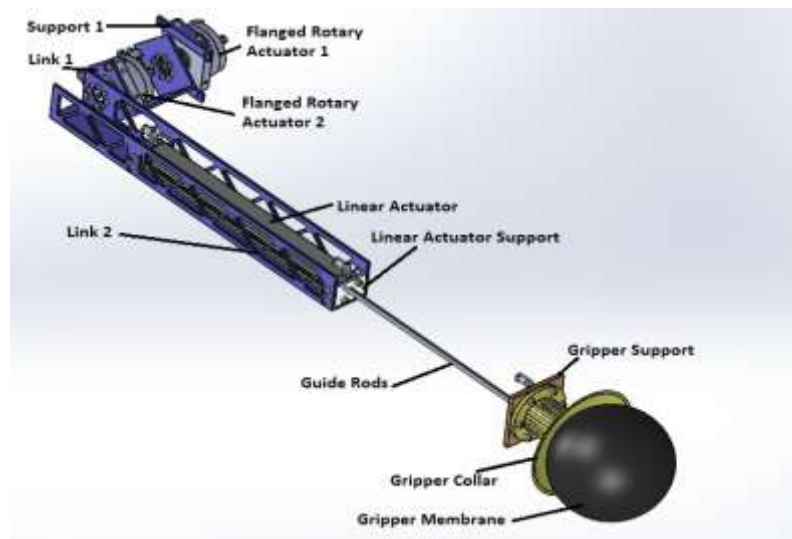


Figure 41: CAD model of Enhanced Manipulator Design 2.5 in a Forward Extend Position



Figure 42: Manipulator Configurations mounted on AUV- Forward, Downward and Keeping Positions

4.2.2. Limitations of Design 2.5

Upon thorough evaluation of Design 2.5, the following limitations were observed:

- 1) This design was based off a smaller rotary actuator which provided insufficient torque for the application. The correct actuators were found to be too huge, bulky and heavy (~5kg) for use.
- 2) The protection purpose of link 2 is made redundant as the linear actuator is hardy enough to withstand impacts should there be any side collisions.
- 3) The diameter of the holes in the linear actuator where the guide rods slide through is non-uniform (Fig 43), thus the guide rods are not very useful.

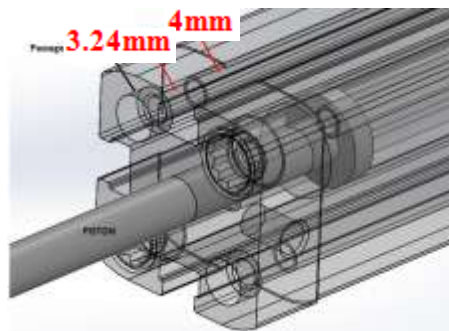


Figure 43: Non-uniform Diameter in Guide Rod Passages within Linear Actuator

4.3. Design 3

To address the limitations of previous designs, modifications were incorporated once again to produce Design 3 (Fig 44), a 2DOF arm that features a shortened Link 1 bolted to the linear actuator, which is then attached to the end-effector via the threaded piston and a T-slot replacing the guide rod. The servo actuation method is re-introduced to replace the rotary actuator, because it is lightweight option and the gearing can be modified provide a high torque. Here, 1 servo is used to actuate the arm and it is housed in a waterproof T6-6061 Aluminium enclosure connecting to the arm via a shaft and a clamp.

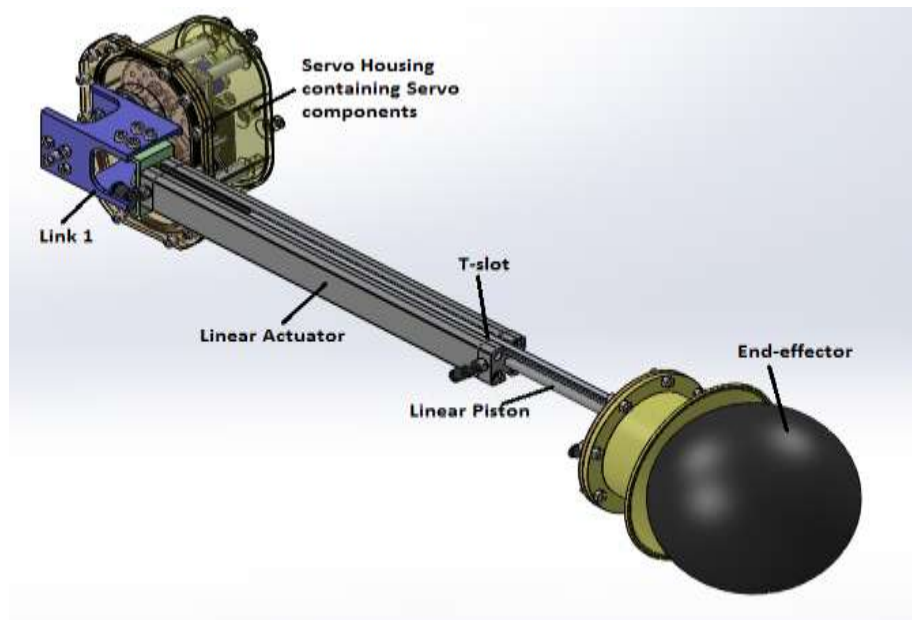


Figure 44: CAD model of Manipulator Design 3 in a Forward Retracted Position



Figure 45: Manipulator Configurations mounted on AUV- Forward, Downward and Keeping Positions

Based on the torque requirements as shown by the torque calculations in Appendix 11, at least 4.9 Nm is required. Hence, the Hitec HS-7950TH high torque servo motor is chosen, which provides an output torque of 17.2 Nm when a two gear combination of size 1:5 (Pinion gear: Hub gear) is used at an applied voltage of 7.4V. The gear relationship is given below:

$$\frac{T_1}{T_2} = \frac{\theta_2}{\theta_1} = -\frac{N_1}{N_2} = \frac{\omega_2}{\omega_1} = -\frac{r_1}{r_2} = -\frac{D_1}{D_2} = GR$$

θ_1, θ_2	angular position of gear 1 and 2, respectively
ω_1, ω_2	angular velocity of gear 1 and 2, respectively
T_1, T_2	applied torque of gear 1 and 2, respectively
N_1, N_2	number of gear teeth on gear 1 and 2, respectively
D_1, D_2	pitch diameter of gear 1 and 2, respectively

Figure 46: Gear Relationship (DesignAerospace, 2016)

By default, the maximum angular position of a servo is 180°. According to the gear relationship, this causes the output angular position to decrease to 36°, which is insufficient for the application. To achieve a 180° rotation on the Hub gear, the Pinion Gear needs to spin

900°. Thus the servo was mechanically modified to remove the mechanical stoppers on the gears and potentiometer, resulting in a continuous rotation servo.

To achieve precise positioning, an optical slotted optocoupler (Fig 47, left) was selected to stop the motor at the correct location using the basis of hole-counting on the Hub gear. A slotted optocoupler is a device comprising a photoemitter (i.e. LED) and a photodetector (i.e. Photodiode) such that the photoemitter always illuminates the photodetector, unless an opaque object enters the slot between them and breaks the beam. Thus in the same way, by the number of times the beam is received it can count the number of holes it passed, enabling the position to be determined. One flaw of this method is the stop reaction time, where the gear will slow down over a distance before coming to a stop, inevitably causing the 180° position to be overshoot. Hence, at the keeping position where it is essential to stop the motor immediately due to the possibility of knocking the thruster when overshooting, a limit switch (Fig 47, right) was selected. A bolt placed on the gear that comes into contact with the hinge at the 0° mark clicks the switch off and stops the motor from further rotation. Supporting mounts as seen in Fig 48 are 3D printed to hold them in place.



Figure 47: Left - Optek Slotted Optocoupler (RS Components, 2016), Right - Basic Limit Switch (Omron, 2016)

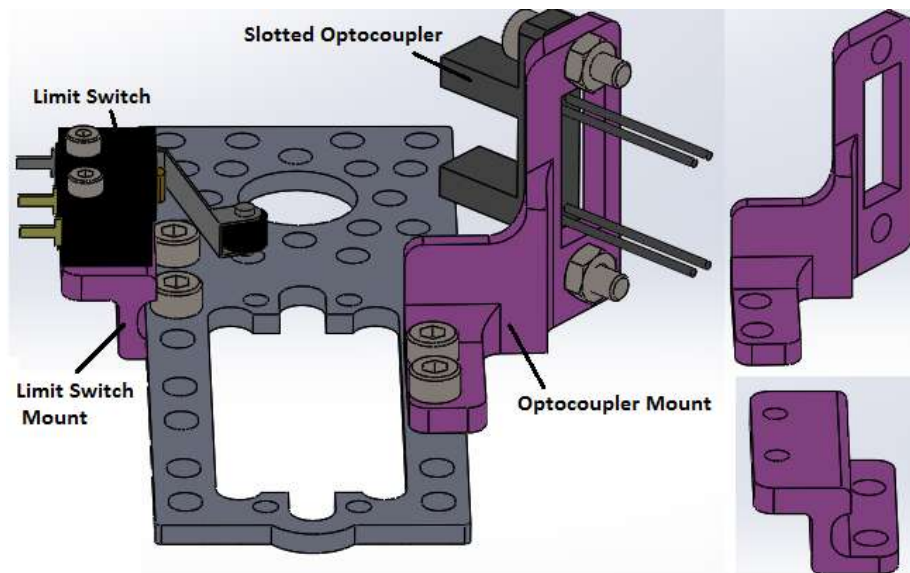


Figure 48: CAD Model of Optocoupler Mount and Limit Switch Mount

Fig 49 shows the assembly of the servo motor, optical and limit switches, gears and the shaft clamped together on the servo stand. The servo stand will be bolted upright and enclosed within a customized servo housing made of corrosion resistance Al T6-6061 shown in Fig 50.

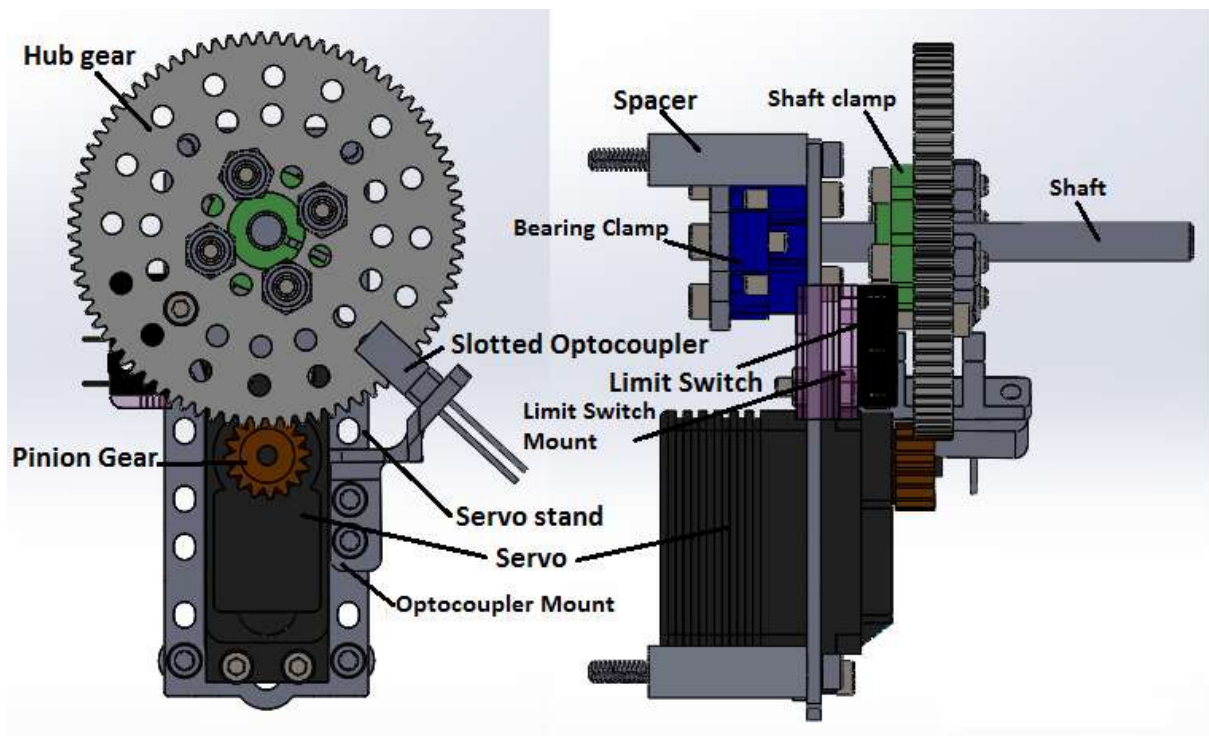
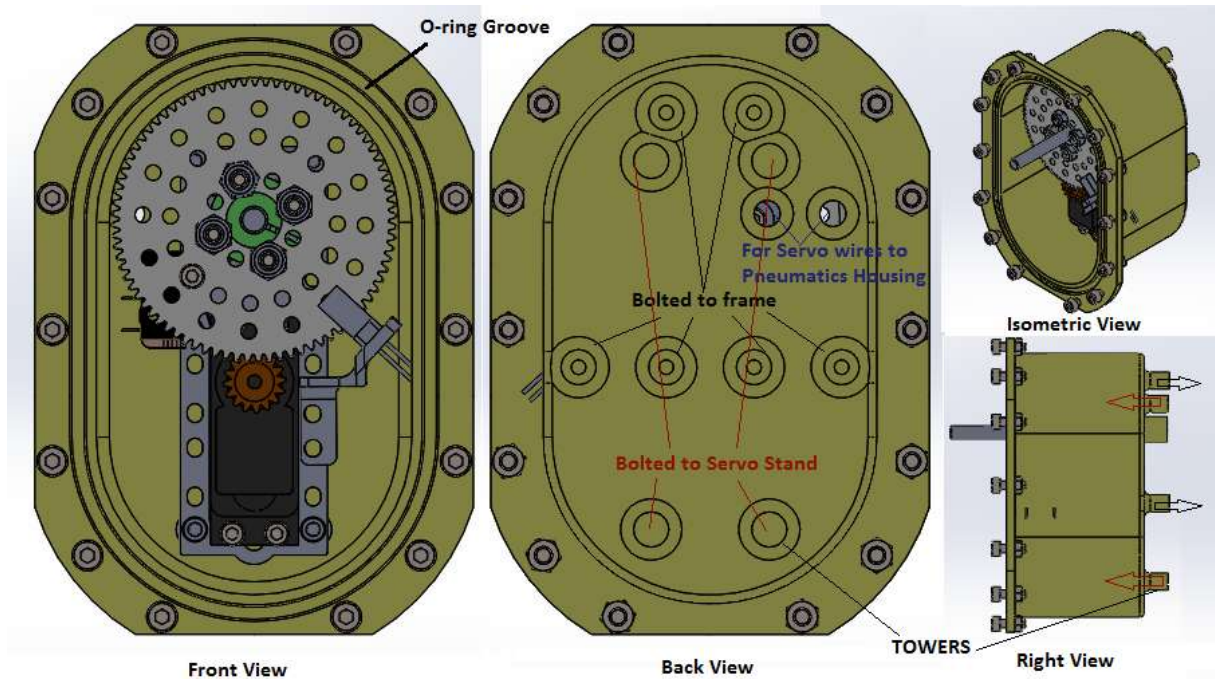


Figure 49: Servo Setup with a 5:1 Gear Ratio to Step Up the Torque



[Figure 50: CAD model of Servo Housing](#)

As can be seen in Fig 50, the servo housing is of a unique oval shape to minimize unused space inside the housing and so reduce overall weight. On the back of the housing, there are towers protruding for various purposes without increasing the amount of material significantly – one is to stably bolt the servo stand on the housing, the next is to bolt the housing on the vehicle frame, and the third is to connect the waterproof tubing to the pneumatic hull which will contain the servo wires.

The sealing of the servo housing is done via compressing a static face seal o-ring with an Aluminium lid, and sealing the shaft dynamically via an AVSLD rotary seal retained in place by a smaller Aluminium lid (Fig 51). This static sealing also influenced the shape of the housing, as Parker recommends the radius of the inside edge of the groove to be at least 3 times the cross-section of the seal (*Parker FAQ*, 2016). Meanwhile, the dynamic seal for the motor shaft is provided by a spring-energized PTFE rotary seal (Appendix 12). Such seals have a U-shaped lip seal with a canted-coil spring that creates a sealing force energized under

dynamic conditions. They are also pressure rated to 200 bar, well within the operational and costs limits for this project. Alternative dynamic seals would need to be applied for deeper applications.

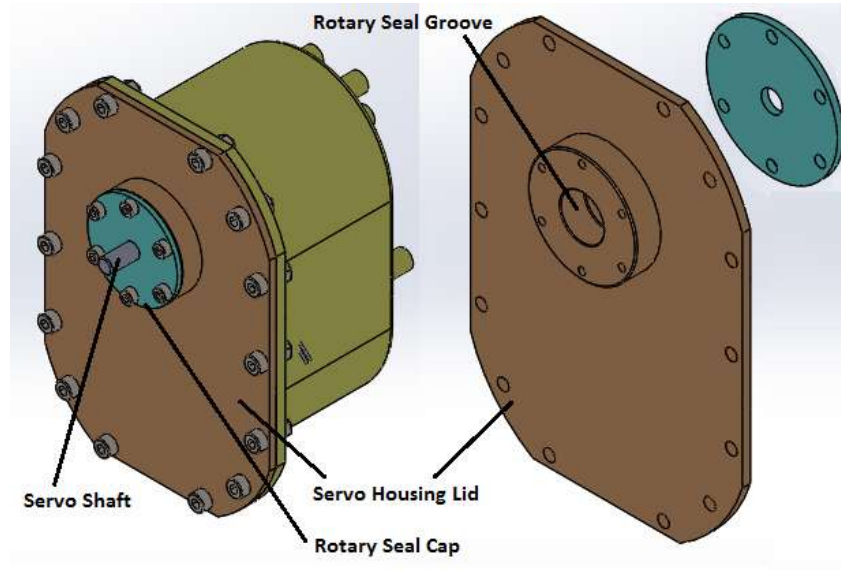


Figure 51: CAD model of Servo Housing Lid and Rotary Seal Cap

Next, the servo is connected to the arm body via the shaft clamped to Link 1, which is then connected to the linear actuator (Fig 44). The main purpose of the linear piston of stroke 250mm is to extend the arm sufficiently to keep within the field of vision (FOV) of the front camera while performing forward tasks (Fig 52), with Link 1 making up for the shortfall in length. Although the arm does not fall within the FOV of the bottom cameras, the offset position of the arm from the localised object can be taken into consideration during grabbing. The FOV of Bumblebee AUV's vision cameras, the Guppy Pro F046C as the front camera and Guppy F146C as the bottom camera, is 70.8 degrees horizontally and 56.1 degrees vertically. Also, both piston and Link 1 enables a clearance of at least 50cm from seafloor to the navigational sensor (i.e. DVL) when performing bottom grabbing tasks to prevent interference of the sensors (Fig 53), as aforementioned in Section 1.2.

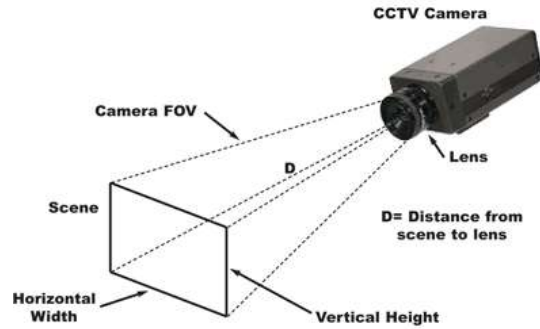


Figure 52: Field of View of a Camera (longrangecamera.com, 2015)

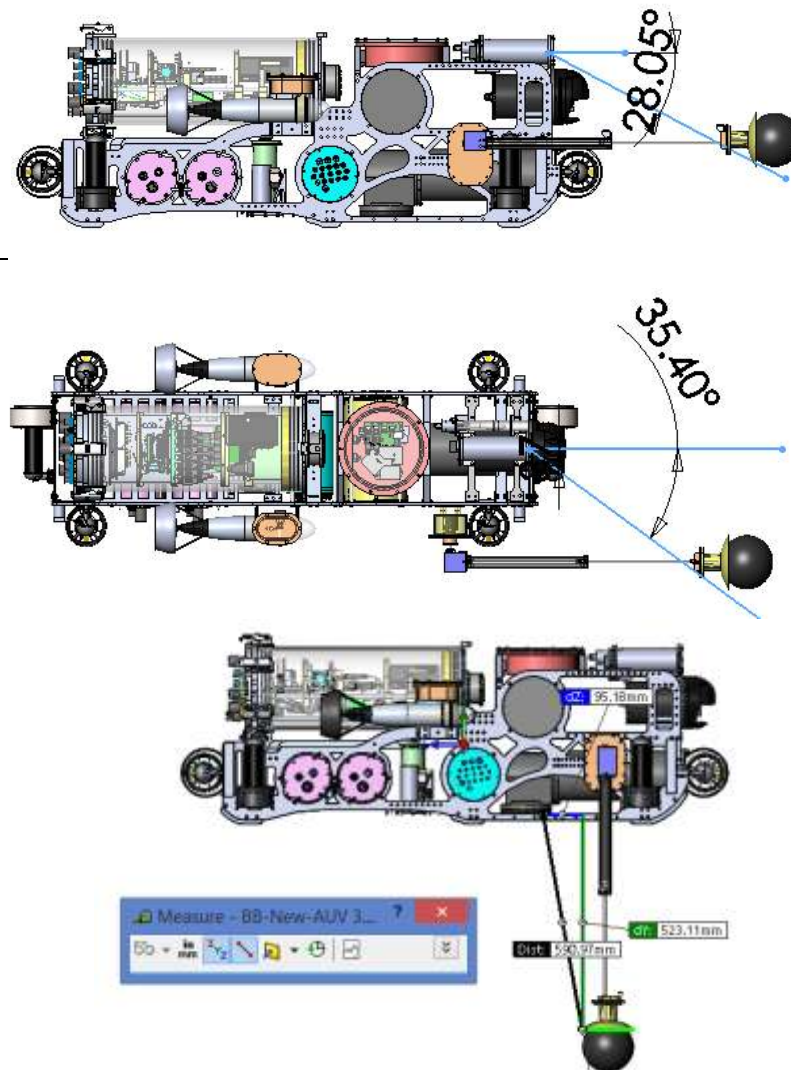


Figure 53: Top - CAD of Forward Manipulator Position within the FOV of the Front Camera, Centre - Forward Manipulator Position within the FOV of the Front Camera, Bottom - Minimum Clearance from DVL to the Seafloor

Additionally, to address guide rod limitations of Design 2, a T-slot component was designed to specially fit into the unique groove of the linear piston (Fig 54). On one end, it has a threaded hole to fit in a 3mm threaded pin which is also bolted onto the end-effector. As the linear actuator extends and retracts during operation, the T-slot slides along accordingly.

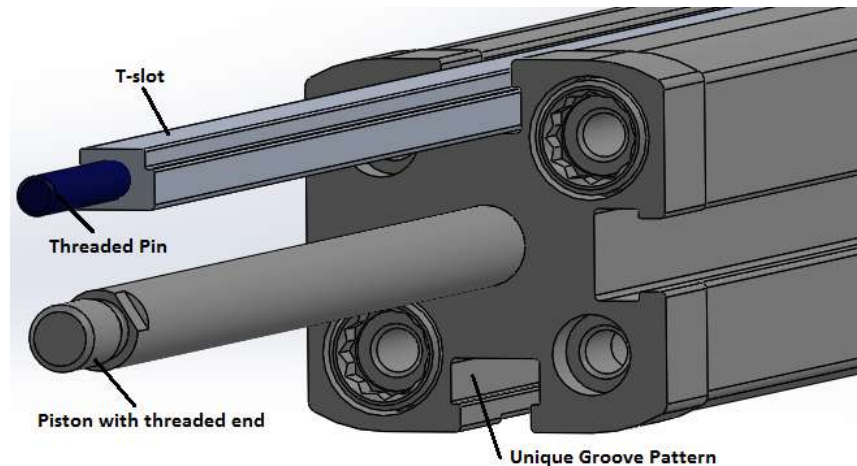


Figure 54: CAD model of T-slot Guide Rod on Linear Actuator

4.3.1. Finite Element Analysis (FEA)

Finite Element Analysis (FEA) was performed using Solidworks Simulation to ensure that the deformation and strain does not exceed the yield value which will result in failure. This allows design improvements to be made before fabrication stage. It was carried out on the more critical parts which bear the greatest weights of the manipulator and they were identified to be the Servo housing, shaft, and Link 1.

Firstly, the Servo Housing towers through which the manipulator is bolted to the vehicle supports the greatest weight of the manipulator. The maximum loading on the housing is 15.0 N on the towers where the manipulator is bolted to the vehicle frame, and 10.6 N on the towers where the servo stand is bolted to the internal housing wall. It was discretised into 12841 elements and the following results were generated (Fig 55).

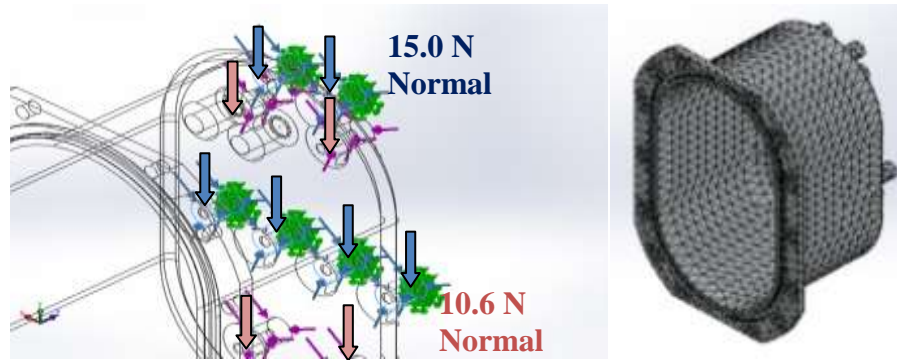


Figure 55: Left - Applied Forces on Servo housing, Right - Meshed Servo Housing

The maximum stress acting on the towers reached up to a value of 0.0302 MPa as indicated by the red sections, far from the Yield Strength of 275 MPa, giving a reasonably high safety factor (Fig 56). Meanwhile displacement was negligible as seen from Fig 57.

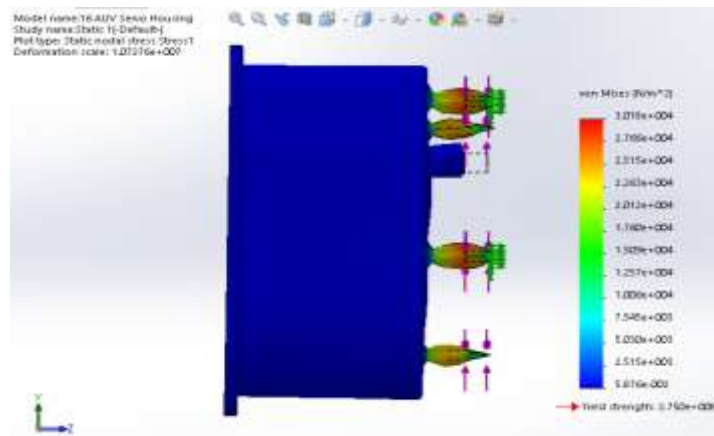


Figure 56: Servo Housing Static Stress Plot

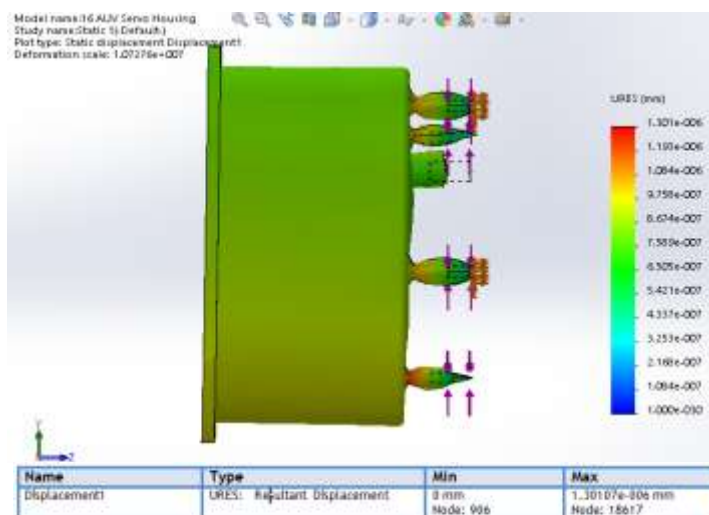


Figure 57: Servo Housing Resultant Displacement Plot

Next, Link 1 was also chosen for FEA as it not only bears a great weight, but also because much material is removed from it, this makes the link very susceptible to failure. The loads acting on the link are calculated to be a normal force of 10.2N, a shear force of 11N, and a bending moment of 4.9Nm about the dotted axis as shown in Fig a. Link 1 was then discretised into 16518 shell elements and the following results generated (Fig 58).

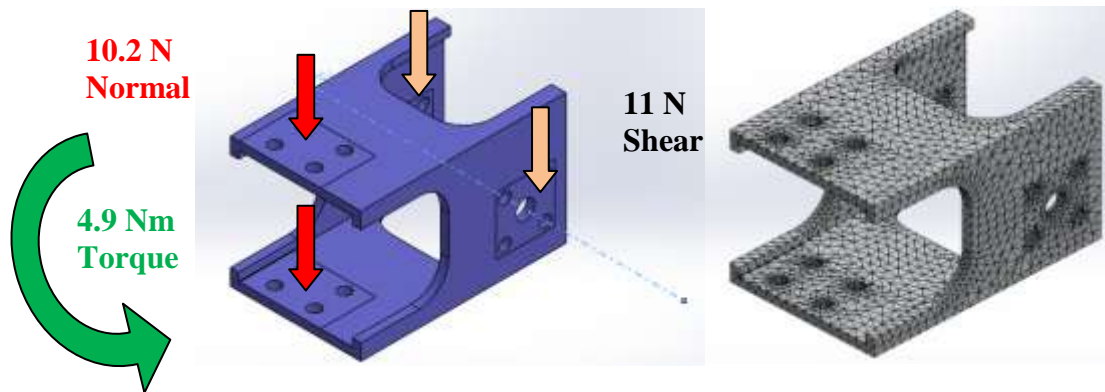


Figure 58: Left - Applied Forces and Torque on Link 1, Right - Meshed Link 1

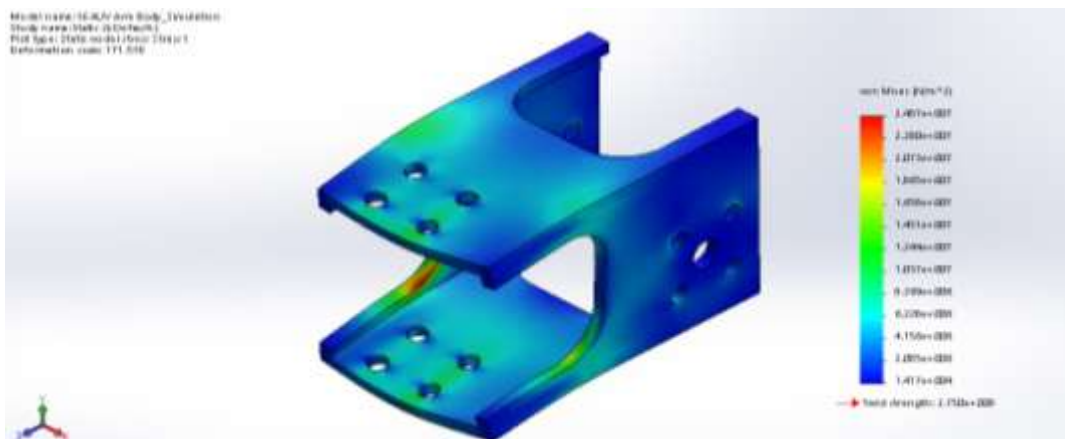
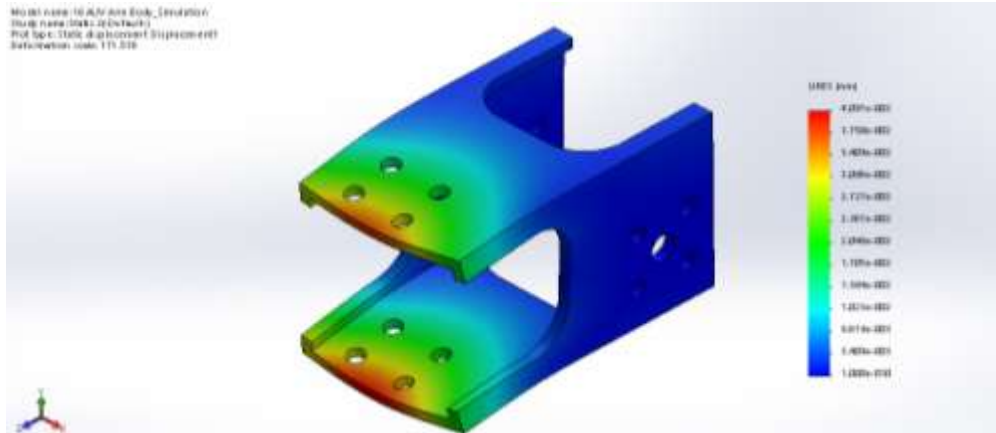


Figure 59: Link 1 Static Stress Plot

Fig 59 shows the stress distribution to lie mainly within the blue regions of approximately 4.15 MPa (<275 MPa Yield Strength), giving a high safety factor. The highest stress as seen by the red spot around the corners is 24.8 MPa, giving a reasonable safety factor of 11. Meanwhile, maximum displacement as seen in Fig 60 remains low and acceptable at 0.041mm at the tip of Link 1.



Name	Type	Min	Max
Displacement1	URES: Resultant Displacement	0 mm Node: 420	0.0409121 mm Node: 1759

Figure 60: Link 1 Resultant Displacement Plot

Finally the Shaft, made of SS303, is a cantilever here with loading on two points amounting to 10.7 N which directly supports Link 1 (Fig 61), making it probable to failure from excessive deformation or fracture. It was meshed with 6730 elements and following results generated.

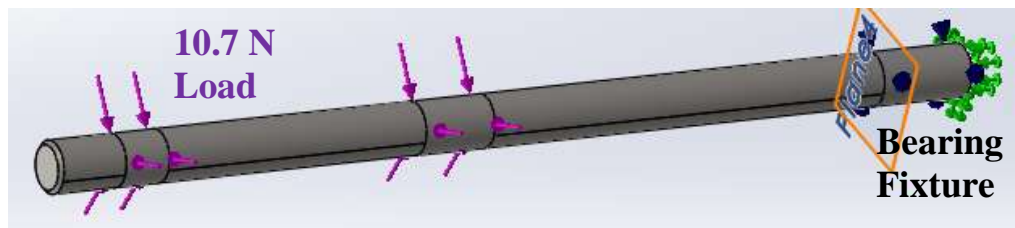


Figure 61: Forces applied on Shaft

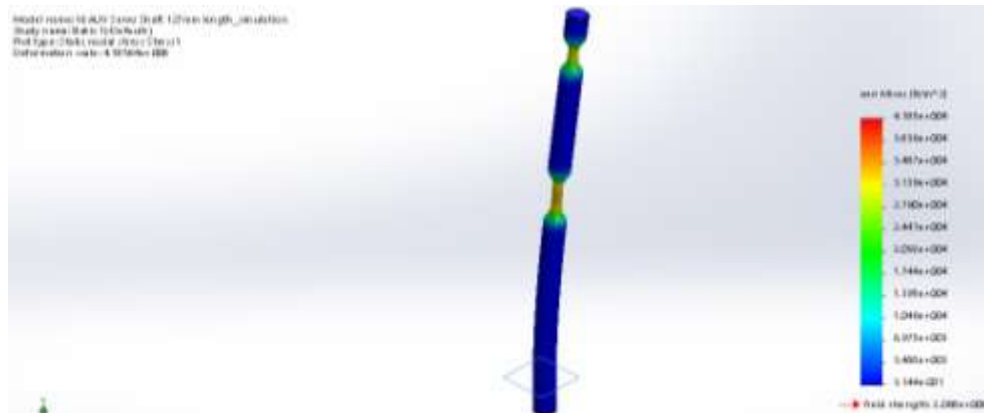


Figure 62: Shaft Static Stress Plot

Results (Fig 62) showed the loading points to face a maximum stress of 0.0342 MPa, much lower than the yield strength of 303 Stainless Steel which is 207 MPa. Also, a low and acceptable maximum displacement of 3.47275e-6 mm is encountered at the free end (Fig 63).

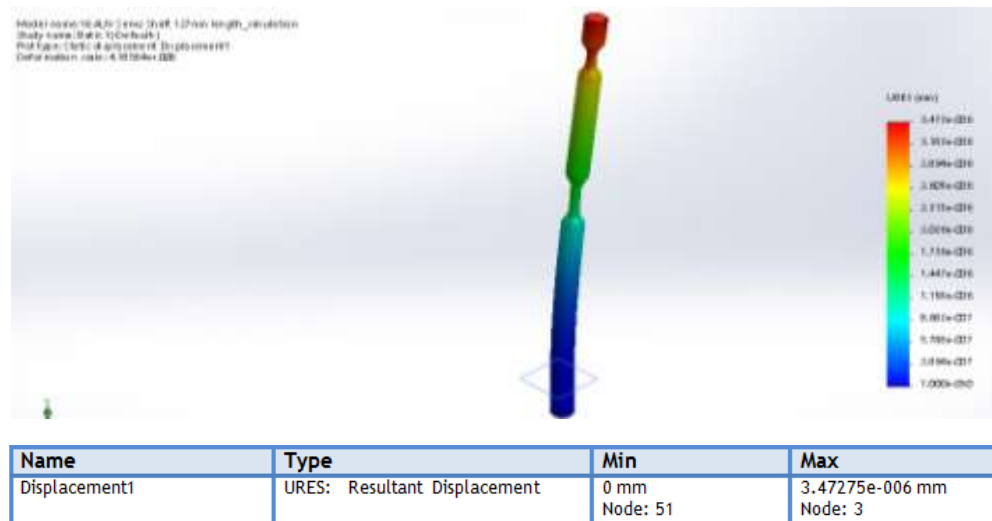


Figure 63: Shaft Resultant Displacement Plot

4.3.2. Computational Fluid Dynamics (CFD)

Computational Fluid Dynamics (CFD) is a method of applying to a simulation mathematical models that describe the fluid properties and behaviour while in motion, and it is carried out using the Solidworks Flow Simulation software. It allows one to visualize and predict how the fluid affects the design in terms of pressure drop, flow trajectories and drag forces exerted etc.

The flow was analysed on three key manipulator configurations - the forward, bottom and back-facing positions. A velocity flow of 1.5m/s was passed over the manipulator along the various axis, simulating the typical vehicle speed and also the typical velocity of currents in the open sea (Coastalwiki.org, 2016). The following results were generated.

The first simulation as shown in Fig 64 represents the manipulator in the downward facing position, with a 1.5m/s flow along the Y-axis, to test its ability to withstand strong currents

when picking an object from below while stationary. The flow is relatively consistent at 1.5m/s over the entire body with negligible flow separation or turbulent flow, and fastest flow of 2m/s visible at the gripper-object interface. The maximum resultant drag force is a value of 15.1 N which will cause a maximum torque of 5.8 Nm about the X-axes (Fig 65), which can be well managed by the servo which can resist 17 Nm (See stall torque under Appendix 12). Meanwhile, pressure distribution (Fig 65) is constant throughout the entire body excluding the servo housing and gripper with a small pressure drop of about 1 kPa around the servo housing and gripper interface.

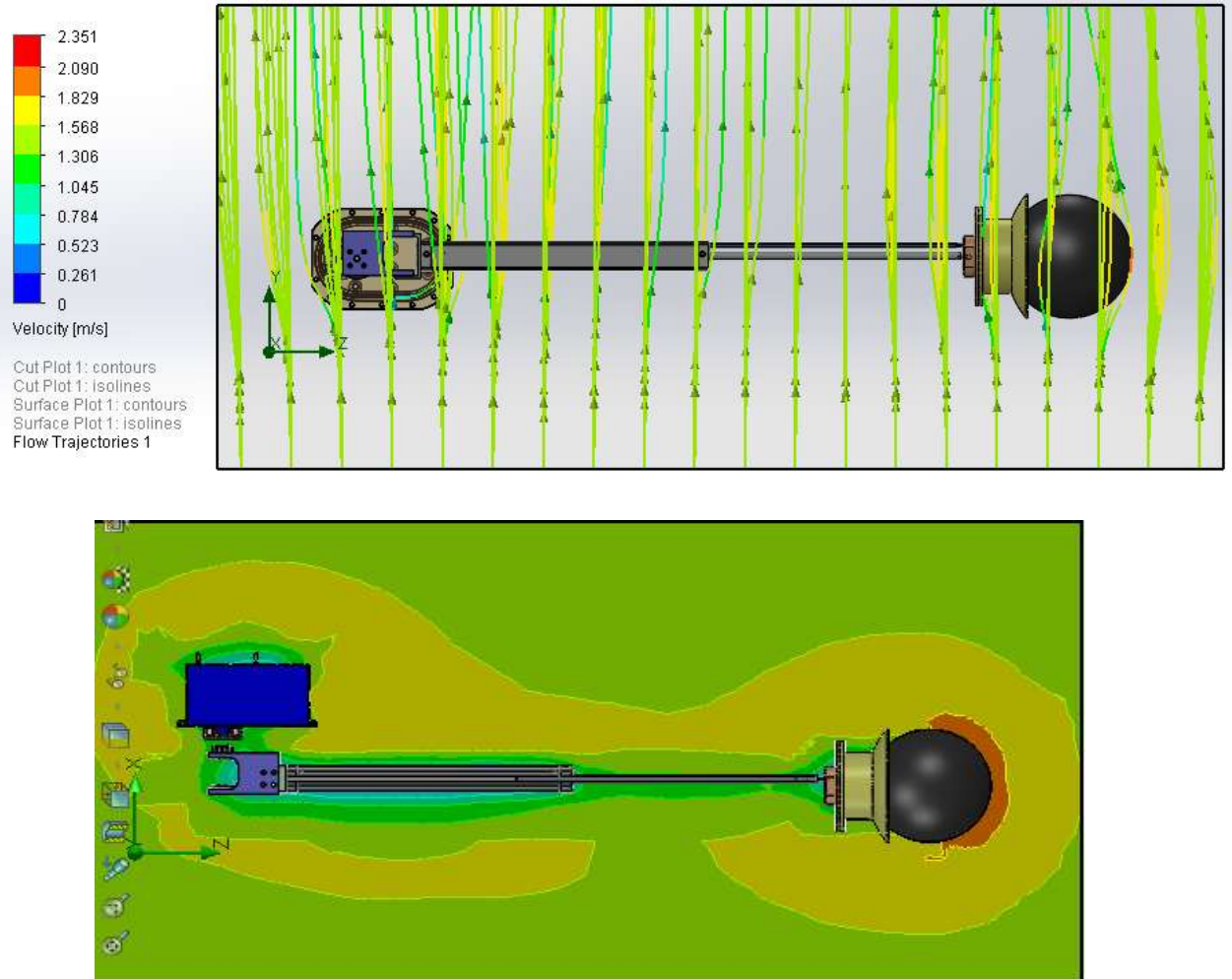


Figure 64: Flow Simulation Results for Currents Flow of 1.5 m/s

16 AUV Manipulator.SLDASM [Project(1) [Default(1)]]									
Goal Name	Unit	Value	Averaged Value	Minimum Value	Maximum Value	Progress [%]	Use in Convergence	Delta	Criteria
GG Max Dynamic Pressure 1	[Pa]	1041.611308	1039.372151	1023.795744	1045.61729	100	Yes	21.82154618	77.46011259
GG Torque (X) 1	[N*m]	-5.763861701	-5.790280962	-5.8417940	-5.763861701	100	Yes	0.077932334	0.36694554
GG Torque (Y) 1	[N*m]	-0.211927986	-0.160258005	-0.268277022	-0.107400315	100	Yes	0.069262255	0.094829998
GG Torque (Z) 1	[N*m]	1.389169317	1.38471299	1.369151485	1.406165236	100	Yes	0.037013751	0.095449311
GG Force (X) 1	[N]	0.304586751	0.529841084	0.304586751	0.606270115	100	Yes	0.132494326	0.158258189
GG Force (Y) 1	[N]	14.82079066	14.95506712	14.820790	15.12600033	100	Yes	0.305209667	1.055024662
GG Force (Z) 1	[N]	1.697222244	1.679590891	1.579805338	1.740610243	100	Yes	0.160804905	0.292744553
Iterations []: 49									
Analysis interval: 21									

Figure 65: CFD Results For Manipulator in Bottom-Facing Position

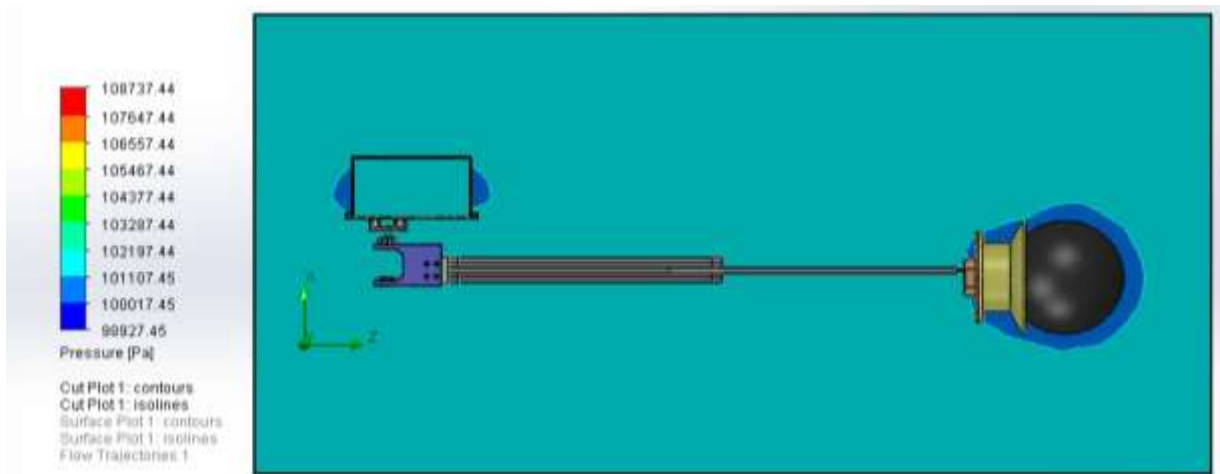


Figure 66: Pressure Simulation Results for Currents Flow of 1.5 m/s

The second simulation is performed on the manipulator in retracted lock position to analyse the significance of the drag forces on the manipulator when the AUV is in forward motion, represented by a flow of 1.5m/s along the positive Z-axes (Fig 67). The flow trajectory reveals some flow separation to occur at the servo housing and gripper-object interface which increases drag forces which is revealed to amount to 15.8Nm (Fig 68). However, the manipulator will not be largely affected as the bulk of the body is streamlined and there is still a non-zero fluid flow along it.

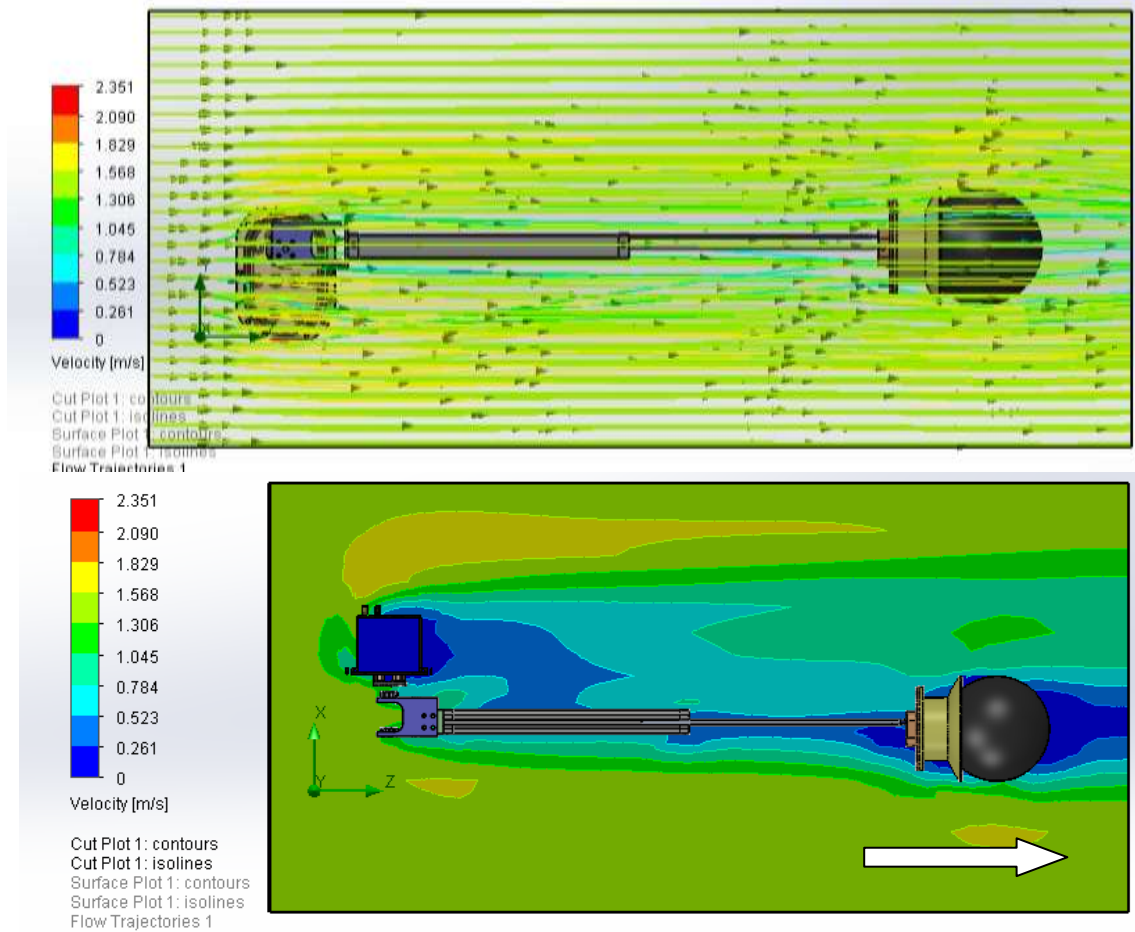


Figure 67: Flow Simulation Results for Forward AUV Motion of 1.5 m/s

16 AUV Manipulator.SLDASM [Project(1) [Default(1)]]									
Goal Name	Unit	Value	Averaged Value	Minimum Value	Maximum Value	Progress [%]	Use in Convergence	Delta	Criteria
GG Max Dynamic Pressure 1	[Pa]	2792.190502	2919.385507	2784.035469	3068.798963	100	Yes	135.5274283	212.8646757
GG Torque (X) 1	[N*m]	0.697728921	0.729641953	0.684501918	0.809428324	100	Yes	0.124926405	0.160910465
GG Torque (Y) 1	[N*m]	-2.617910886	-2.795276607	-3.032781823	-2.611736294	51	Yes	0.215816202	0.110192168
GG Torque (Z) 1	[N*m]	-0.021746828	-0.006567825	-0.02930254	0.017854201	100	Yes	0.015006263	0.019798922
GG Force (X) 1	[N]	-1.558126739	-1.770337747	-2.076227734	-1.52687044	100	Yes	0.239619175	0.298275566
GG Force (Y) 1	[N]	-0.282408183	-0.336563174	-0.447636559	-0.270064128	42.1	Yes	0.170868376	0.072095021
GG Force (Z) 1	[N]	15.75678408	15.70401312	15.67513288	15.75678408	100	Yes	0.081651201	1.110138723
Iterations []: 181									
Analysis interval: 23									

Figure 68: CFD Results For Manipulator in Keeping Position

Finally the third simulation is carried out while the manipulator is in a forward grabbing position to assess how much the actuation capabilities will be affected by drag forces, as represented by a 1.5m/s flow along the negative Z-axes. The following flow trajectory (Fig 69) revealed the flow separation to occur along the linear piston and gripper, resulting in

maximum drag forces of 12.5N (Fig 70). However, the drag force is insignificant in hindering the linear actuation of the piston, which has a thrust force of minimum 51 N at 6 bar compressed air pressure (Appendix 8).

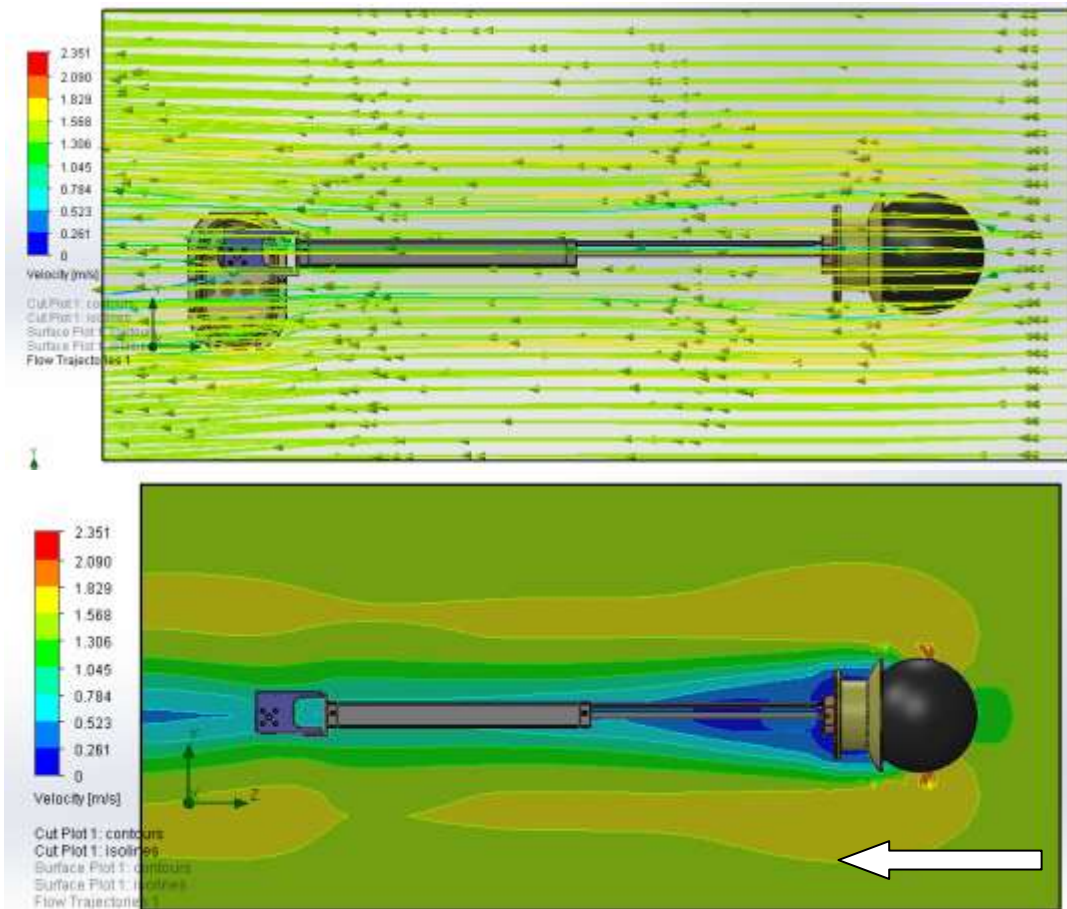


Figure 69: Flow Simulation Results for Forward Actuation Motion in Back Currents of 1.5 m/s

16 AUV Manipulator.SLDASM [Project(1) [Default(1)]]									
Goal Name	Unit	Value	Averaged Value	Minimum Value	Maximum Value	Progress [%]	Use in Convergence	Delta	Criteria
GG Max Dynamic Pressure 1	[Pa]	2031.004649	2030.030562	2014.559086	2055.483713	100	Yes	11.30042006	33.05644702
GG Torque (X) 1	[N*m]	-0.979488603	-0.979078574	-0.99856171	-0.964984605	100	Yes	0.015516596	0.065656025
GG Torque (Y) 1	[N*m]	1.416413968	1.407573831	1.382024876	1.429628184	100	Yes	0.015254301	0.07132413
GG Torque (Z) 1	[N*m]	0.090092816	0.087683316	0.081409712	0.09329224	100	Yes	0.00470338	0.00493777
GG Force (X) 1	[N]	-1.629275068	-1.642338146	-1.697350766	-1.60586522	100	Yes	0.037855542	0.081332174
GG Force (Y) 1	[N]	-0.134442332	-0.153170752	-0.18863809	-0.134442332	100	Yes	0.011852848	0.04034924
GG Force (Z) 1	[N]	-12.45907612	-12.4667004	-12.49507733	-12.43998074	100	Yes	0.028076081	0.643759755

Iterations []: 175
Analysis interval: 27

Figure 70: CFD Results of Manipulator in a Forward Position

5. Electrical Architecture of Manipulator

The Electrical architecture of the manipulator to power and control the electronics (Fig 71) was done in collaboration with an Electrical subteam member from Team Bumblebee. During operation of the manipulator, the arm has to rotate using a modified servo motor, extend via a linear piston towards its target, and activate the vacuum generator to remove the air from the jamming gripper to grab the object. All these components need to be controlled by a dedicated Printed Circuit Board (PCB) that interfaces with the AUV main control system and is also capable of operating independently of the existing systems.

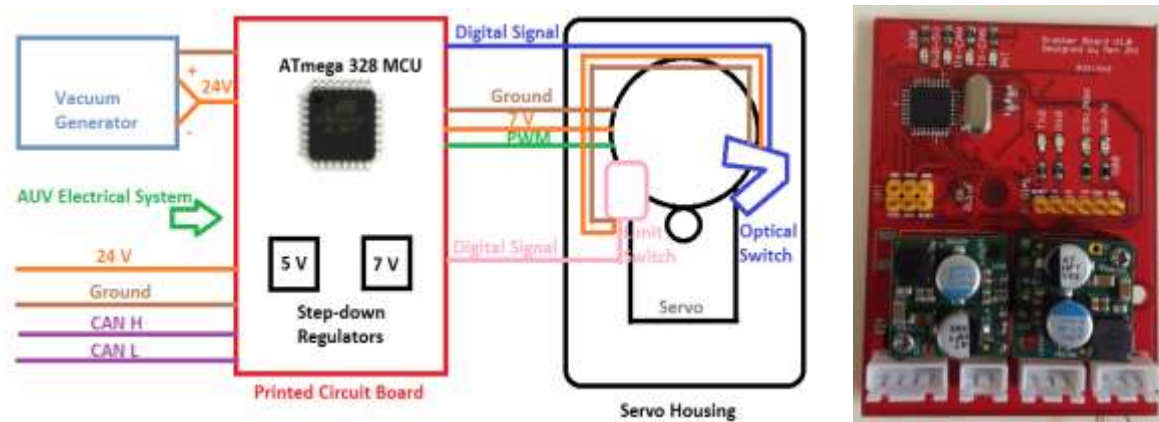


Figure 71: Left -Schematic Diagram of the Electrical Architecture for the Manipulator System, Right - Fabricated Manipulator Printed Circuit Board

Firstly, to turn the continuous rotation servo motor, which has been mechanically modified to allow for high torque characteristics without compromising on the rotation angle, 7V power source and Pulse Width Modulation (PWM) signal are required. Secondly, to detect and control the angle for precise control, the optical switch and limit switch are implemented, and their operating requirements include 7V power source and digital signals. Thirdly, to extend the arm via the linear piston, a solenoid valve needs to be energized by a 24V power source. Finally, to activate the jamming gripper, the vacuum generator is powered by 24V power that

switches between vacuum pulse and release pulse. The entire electrical system is controlled by an ATmega328 MCU chip on the PCB. The MCU and vacuum generator are located in the Pneumatics Housing while the rest of the electrical components are in the Servo Housing, with cables enclosed within Pneumatic tubes to keep it waterproof.

6. Assembly and Testing of Manipulator

6.1. Testing in Air

The focus of this testing was to verify that the manipulator was able to effectively achieve 180° rotation and stop precisely at the three configurations. The test setup consists of the manipulator, a breadboard because the PCB following the improved design was still under fabrication, and also the power supply. The procedure first involved getting the servo to stop precisely at the 180° , 90° , and 0° angles (Fig 72). Upon success, the manipulator was fully assembled and tested (Fig 73).



Figure 72: Assembly of Servo Components



Figure 73: Assembly of Manipulator

The manipulator was programmed to rotate periodically, without the servo lid so that the spin of the servo gears can be observed. However, contrary to the prediction by the torque calculations, the manipulator was not able to reach the 0° and 180° configurations, but only partially up to 45° and 135° (Fig 74). This is a result of several factors: the slip in the shaft which prevented the arm from lifting up as well as non-uniformly distributed masses and unaccounted weights which resulted in a high bending moment for servo to manage.



Figure 74: Air Trials Results , Left – 45° Configuration, Right – 135° Configuration

6.2. Testing in water

Despite the inability to lift the manipulator in air, plans were made to proceed with water trials, due to the fact that the manipulator weight will be reduced underwater owing to the natural buoyancy of several components, namely the granular membrane and the Servo housing which contains an air pocket. The importance of the water trial was also to test the entire gripping procedure, involving the manipulator rotation, linear actuation, granular jamming and picking of objects, as well as the release and placement of objects.

From the pool test (Appendix 13), it is discovered that the arm is positively buoyant in water, hence this will aid the motor in lifting the arm up. Next, the gripper proceeded to pick up and

place objects of various structures and weights, and was successful in picking up a sphere, cylindrical PVC pipes, heavy items such as 2-pearls weight, small items such as a screwdriver head, and soft items such as a kickboard and various floats. What the gripper was unsuccessful in was lifting up were floats of a higher porosity and decreased hardness, as well as a rope. Observations revealed that the reason was because the gripper could not sufficiently wrap around the object for geometric interlocking gripping mode and object porosity disallows for the suction gripping mode.

7. Results and Discussions

This section serves to emphasise on the characteristics for this manipulator design, a high torque servo-run Jamming Gripper, to succeed in reliable manipulation underwater, as well as to highlight some of the limitations that can be improved in future designs. Based on the results and observations of the earlier trials on both the manipulator arm and jamming gripper, the characteristics for efficient gripping can be summarized as follows:

- 1) A mixture of both Coarse and Fine Coffee grains to be used as the granular materials for high gripping strength and conformability to object surface
- 2) High Vacuum Percentage in the Jamming Gripper
- 3) A Shallow and Wide gripper cup for optimization of grains
- 4) A Large Granular Membrane to surround at least 75% of surface for smooth cylindrical or spherical objects i.e. PVC pipes for firmer grip through Geometric Interlocking Gripping Mode
- 5) A Continuous Rotation Servo to achieve multiple configurations
- 6) Good to grip spherical or angular, small, odd-shaped objects

- 7) A Lightweight Manipulator, or/and a Manipulator Form that does not weigh down directly on the servo motor, or/and High Torque coupled with High Current Supply

However, the aforementioned characteristics also bring about several limitations. Suggestions are also brought up on how these limitations could be addressed.

A) Requirements for a Large compressed air tank

A separate trial revealed that the current air tank capacity only allows for 6 attempts of pick-and-place before being drained out, which is too few an attempt for competition use or real world applications. More air is required and further reduces this number especially when the depth increases and the surrounding water pressure is significant. A larger air tank would be required but this will also reduce the space and payload of the underwater vehicle for other important sensors.

Thus, in deep water applications, rather than using air as a medium within the jamming gripper, a chemically inert fluid and a coarse and fine mix of glass beads could be employed instead to make up the jamming gripper. Then, a pump used to circulate this fluid in and out of the gripper for jamming within a closed loop system has to be carefully sourced for.

B) Possible Damage to Servo and Inhibition of Servo Performance

In this case, the standard servo was mechanically modified to achieve the required angles through removal of the physical stoppers without hacking the firmware of the Servo, resulting in the loss of some of its basic functions such as speed variation and precise positioning. As the firmware of such servos is not modifiable, in future a stepper motor with a similar gearbox setup could be used instead to achieve the high torque while retaining its precision and speed.

C) Manipulator Type

This type of manipulator arm is not very efficient because the weight of each component that make up this manipulator are exerted directly on the servo, and it is further compounded with length to create a high resistive torque on the servo. What could have made a more efficient manipulator would be one that has the base or heaviest portion of the manipulator mounted and supported by the vehicle frame rather than by the servo. Therefore, the plans for future new AUV designs must be done in sync with the manipulator design, so as to set aside a suitable location for the manipulator and reduce such inefficiencies.

8. Conclusions

In this project, a pick-and-place manipulator has been designed, prototyped, built, tested and integrated while working on the constraints of an existing design as well as competition requirements. Initially, the design was cadded out using Solidworks, checked via Solidworks FEA and CFD as well as through the prototyping of 3D printed materials, with iterations being made to further improve the design. After successful trials on the jamming gripper, the design was proceeded to be machined. After fabrication was done, the mechanical components were test-fitted and assembled, before integration with the electrical systems. Finally, testing of the manipulator was conducted to check the effectiveness and functionality, to which the results have not been completely ideal, and so thoughtful propositions were raised on how future designs can be improved.

9. Recommendations for Future Works

The current manipulator can be improved generally in terms of mechanical design, form factor, weight and size reduction, and the choice of materials or components used.

For the arm, light composite materials that give a high strength, such as carbon fiber, could be explored as a possible choice of material for the arm. Other methods of actuation, like stepper motors could also be explored and tested. Also, the efficiency of the manipulator can be enhanced if the weight is mainly supported by the vehicle frame, and if the design of the manipulator is planned in conjunction with the subsequent AUV design.

Last but not the least, the reliable success of a jamming gripper in pick-and-place applications in water has highlighted its potential in underwater environments. The type of membrane and grains could be custom-made with carefully selected properties to enhance gripping performance in the water. Also, to minimize the consumables required during gripping, further research could be pursued on the use of a chemically inert liquid as the medium in place of air for jamming, and how the closed loop system could have been designed. Finally, the effects of the jamming gripper integrated onto the AUV using computer vision can be studied. This will pave the way for a robust and versatile gripping technique for future underwater intervention technologies.

Appendices

Appendix 1 – Figure 75: Official Competition Rules for SAUVC 2016 and Robosub 2016

SAUVC Rulebook

4. Specification of AUV

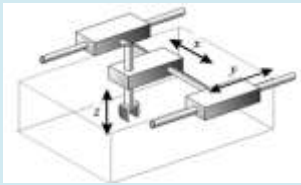



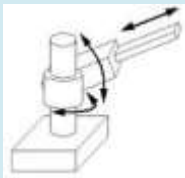
- The AUV must fit within a 140 × 100 × 100 cm box.. An AUV with dimension of less than 70 cm × 50 cm × 50 cm will be given bonus [10 points].
- The AUV must not weigh more than 50 kg in air. An AUV weighing less than 40 kg in air will be given bonus **[10 points]**.
- Power should be self contained. Tethers of any sort are not allowed.
- The voltage of the power source used by each AUV should not exceed 24VDC.
- Pressure of any compressed gas used must not exceed 6 bars.
- AUV should be completely autonomous. No communication of any sort is allowed during the game
- The use of explosives, fire or hazardous chemicals is prohibited. Certified lithium batteries are allowed
- If lasers are used, they must be of class 2 or lower. Care must be taken to protect all persons at the venue from harm. Beams must be oriented in such a fashion that they cannot shine into the eyes of the spectators.

5.2.Weight and Size Constraints

For the RoboSub competition, each entry must fit within a six-foot long, by three-foot wide, by three-foot high “box” (1.83m x 0.91m x 0.91m). Table 1 shows the bonuses and penalties associated with a vehicle’s weight in air

Table 1: Vehicle weight in air with Bonus or Penalties		
	Bonus	Penalty
AUV Weight > 125 lbs (AUV Weight > 56.7 kg)	N/A	Disqualified
125 lbs ≥ AUV Weight > 84 (56.7 kg ≥ AUV Weight > 38)	N/A	Loss of 250 + 5*(lb – 125) 250 + 11*(kg – 56.7)
84 lbs ≥ AUV Weight > 48.5 (38 kg ≥ AUV Weight > 22)	Bonus of 2*(84 – lb) 4.4*(38 – kg)	N/A
AUV Weight ≤ 48.5 lbs (AUV Weight ≤ 22 kg)	Bonus of 80 + (48.5 – lb)	N/A

Appendix 2 - Table 1: Characteristics, Advantages and Disadvantages of Manipulator Types (Kuttan, 2007) & (Circuitdigest.com, 2015)

Manipulator Types & Characteristics	Advantages	Disadvantages
Cartesian Manipulator - 3 prismatic joints - Linear movements along 3 principle axis 	- Can perform straight-line insertions - Easy to program - Almost independent of gravity and collision with objects	- Occupies too much space - Less accurate resolution
Selective Compliance Articulated Robot Arm (SCARA) - Comprises a shoulder, elbow joint and wrist axis - 2 revolute joints and 1 prismatic joint 	- Rigid and durable - Good for application which require fast, repeatable and articulate point to point movements (eg. palletizing, and machine loading/ unloading and assembly)	- Relatively inflexible - Limited Movements
Cylindrical Manipulator - Three axes of motion - A circular motion axis and two linear axes - 1 revolute joint, 1 cylindrical and 1 prismatic joint 	- Moves faster than Cartesian Manipulator given the same distance between two points - Rigid - Capacity to carry high payloads	- Requires added transformation from Cartesian coordinate system to cylindrical coordinate system. - Less work volume
Programmable Universal Manipulation Arm (PUMA) - 3 revolute joints, compliant in all three axis X, Y, Z - Main uses in assembly, welding and object handling 	- High flexibility - Huge work volume - Quick Operation	- Relatively low precision
Polar Manipulator - 2 revolute & 1 prismatic joint to make near spherical workspace. - Main uses in handling operations in production line and pick and place robot. 	- Low weight and minimal structural complexity - Large Workspace - Good resolution as errors in the end-effector are perpendicular to one another	- Large and variable torque required - Difficulties in counter-balancing - Limited ability to avoid collision with objects - Large position error due to rotation motion and proportional radius

Appendix 3 - Table 2: Characteristics, Advantages and Disadvantages of Different Actuation Types

Actuation Types and Characteristics	Example	Advantages	Disadvantages
Pneumatic <ul style="list-style-type: none"> - Driven by compressed air, it converts energy into linear or rotary motion. - The pressure and flow of air determines both speed and torque. - Used in applications in which positional accuracy is not a requirement. (Deaconescu, 2014) 	 <p><u>Festo Pneumatic Gripper DHxS series (Control Design, 2015)</u></p>	<ul style="list-style-type: none"> - Has shock-absorbing capacities - Light weight, compact size, reduced mass-to-power unity ratio - Easy adjustment of forces, torques and speeds - Compliant behavior and elastic behavior due to air compressibility and variation of force with displacement. 	<ul style="list-style-type: none"> - Low positional accuracy and flexibility - Requires a steady supply of pressurised air - Has to go full stroke
Hydraulic <ul style="list-style-type: none"> - Consists of a piston movement along a tube using pressurized fluid such as oil or water. - Often used for applications that requires significant amounts of force. 	 <p><u>Schunk hydraulic parallel gripper (Directindustry, 2015)</u></p>	<ul style="list-style-type: none"> - Provides high torque - Can output linear, rotary, or oscillating motion 	<ul style="list-style-type: none"> - Limited acceleration - Heavy - Has to go full stroke - Typically inefficient and requires regular maintenance (Tigertek Industrial Services, 2015).
DC Stepper motors <ul style="list-style-type: none"> - Motors rotate in discrete step increments. - The direction of shaft rotation is directly related to the sequence of the applied pulses, the speed of the motor shafts rotation is directly related to the frequency of the input pulses, and the length of rotation is directly related to the number of input pulses applied. - Used in high-speed motion-control applications. 	 <p><u>Pololu Stepper motors (Pololu.com, 2015)</u></p>	<ul style="list-style-type: none"> - Cost effective - Easy to control, where characteristics of stepper motor rotation can be varied by the applied input pulses (Industrial Circuits Application Note, 2015) 	<ul style="list-style-type: none"> - Provides low torque - Given a certain torque, they are larger and heavier than their servo counterparts - Relatively lower positional accuracy than servos

<p>DC Servo motors</p> <ul style="list-style-type: none"> - Allow continuous rotation providing speed control and position accuracy - Increasingly used in industrial settings because of its ease of control. 	 <p><u>Hitec HS-485HB Servo Motor</u> (Tetrixrobotics.com, 2015)</p>	<ul style="list-style-type: none"> -Small, light - Operationally cost effective in comparison to pneumatic actuators (RobotWorx, 2015). - Flexible and allows accurate position control through detection of the grip which is mandatory for error proofing. - Allows control of gripping force and speed which is helpful for gripping fragile parts (Bouchard, 2015). - No air lines, hence preventing contamination to the environment due to air leakage 	<ul style="list-style-type: none"> - Generally provides low torque
<p>AC motors (induction type)</p> <ul style="list-style-type: none"> - Electric motors operate on the principles of magnetism. They contain a coil of wire and two fixed magnets surrounding a shaft. - When alternating currents (AC) are applied to the coil of wire, it becomes an electromagnet, generating a magnetic field. With the interaction between the magnetic fields of the rotor and stator, the shaft and the coil of wires begin to rotate, operating the motor 	 <p><u>Anaheim Automation's AC Induction Motors</u> (AnaheimAutomation, 2015)</p>	<ul style="list-style-type: none"> - Rotate with constant speeds 	<ul style="list-style-type: none"> -Additional microprocessors are used to provide variable speed capabilities
<p>Vacuum</p> <ul style="list-style-type: none"> -Use a closed-cell foam rubber layer, or a rubber or polyurethane suction cup to pick up items. - Common end of arm tooling (EOAT) in manufacturing or assembly line because of its high level of flexibility (RobotWorx, 2015). 	 <p><u>Fipa Suction Cups (Fipa, 2016)</u></p>	<ul style="list-style-type: none"> -Universal option, can handle a variety of products of various shapes, sizes and materials - Fast, reliable and secure holding 	<ul style="list-style-type: none"> -Require many suction cups to be used at one time, resulting in a large and heavy manipulator -May be inefficient in moist or damp conditions

Appendix 4 - Equations Describing the Three gripping modes (Brown et al., 2010)

d = width of pinched region = 1.07 ± 0.07 mm; σ^* = stress magnitude along which pinched region acts on the object = 50 ± 4 kPa, θ = contact angle to the point where the object is enveloped by the gripper (range: $\pi/4 < \theta < \pi/2$), and μ = coefficient of friction ≈ 1 for rubber.

- 1) The frictional mechanism alone can contribute to a holding force F_h of:

$$F_h = F_f = 2\pi R d \sigma^* (\mu \sin \theta - \cos \theta) \sin^2 \theta.$$

Below a minimum angle $\theta \approx \pi/4$, the gripping strength is insignificant except for a small contribution from residual membrane stickiness. The friction mechanism is found to be operative in all cases - resisting forces in all directions and torques applied at the surface at approximately the same magnitude.

- 2) The suction mechanism enhances the holding force F_h to be:

$$F_h = F_s + F_f = \pi R^2 \sigma^* (\mu \sin \theta - \cos \theta) \sin^3 \theta \left(1 + \frac{2d}{R \sin \theta} \right).$$

For smooth spherical objects, the pinched region of the gripper against the object can simulate an effective O-ring and form an airtight seal which contributes an additional vertical suction force F_s . This gripping scenario also holds a vacuum with pressure P_g in the gap region $\pm \theta$ inside the contact line. The pressure on the pinched O-ring will keep the vacuum seal in place as long as the frictional stress exceeds the gap pressure P_g , $= F_f/A_0 = \sigma^* \sin \theta (\mu \sin \theta - \cos \theta)$. The suction mechanism is operative only in several cases, where it is dependent on the target geometry and force direction.

- 3) The interlocking mechanism contributes a holding force F_i :

$$F_i = \int_{\pi/2}^{\theta} (2\pi R t^2 / l) \sigma(\epsilon) \sin \theta' d\theta'$$

Geometrical interlocking occurs when contact angle $\theta > \pi/2$, where the elastic membrane effectively conforms itself to protruding parts of the object depending on its elasticity. The holding force is dependent on a resistance to both bending and stretching forces exerted on the membrane to enable the object to slip out. F_i captures both the lower and upper limits of interlocking. The minimum contribution from interlocking, i.e. contact angles $\theta \ll \pi/2$, $F_i \approx (\pi/2)ER^2(t/l)^3 (\theta - \pi/2)^3$ is the amount required to bend the ring wrapped around the sphere to vertical so the object can slip out, with t as the thickness of the gripper section wrapped around the sphere and l as the bending arm length. Alternatively, to stretch open the neck of the region wrapped around the object for it to slip through, a force $F_i \approx (ERt/6)(\theta - \pi/2)^3$ is required. The upper limit occurs at high interlocking, i.e. large contact angles $\theta \gg \pi/2$, where large strains are needed to pry open the bag, resulting in

$$F_i \sim (2\pi Rt^2/l)\sigma_f.$$

Appendix 5 – Table 3: Density of Common Granular Materials (Engineering toolbox, 2015)

Material	Density (kg/m ³)	
	From	To
Coffee, ground	-	321
Flour, Corn	481	585
Glass Beads	-	1923
Milk powder	-	320
Salt, granulated	-	1281
Sand	1281	1602
Sugar, granulated	-	849



Figure 76: Different grades of Coffee grains, with increasing coarseness from 1 to 4

Appendix 6 – Table 4: Tabulation of Pre-Experiment Results of 5” Jamming Gripper

Object , Characteristics/Weight (g)		Fine		Coarse		Fine + Coarse Mixture	
		Air	Water	Air	Water	Air	Water
Tweezer, Tip Side	8	✓	✓	✓	✓	✓	✓
Tweezer, Flat Side	8	✓	X	✓	✓	✓	✓
Pen, Cylindrical	16	✓	✓	✓	✓	✓	✓
Pen, Cylindrical+Clip	16	✓	✓	✓	X	✓	✓
Watch	82	✓	✓	✓	✓	✓	✓
Legend: ✓ = Success in picking up X = Failed to pick up							

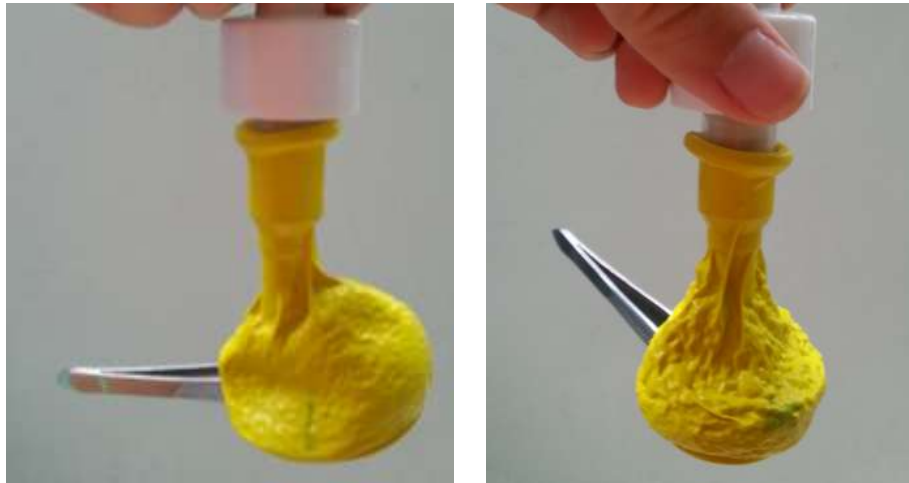


Figure 77: Left - Fine Grain Coffee used to pick up a tweezer by the tip, Right - Coarse Grain Coffee used to pick up a tweezer by the tip

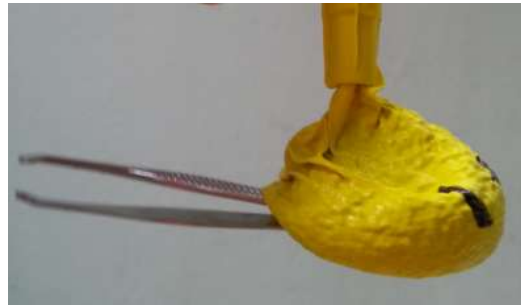


Figure 78: Left - Fine Grain Coffee used to pick up a tweezer by the flat side, Right - Mixture of Fine & Coarse Grain Coffee used to pick up a tweezer by the flat side



Figure 79: Left - Fine Grain Coffee used to pick up a pen by the cylindrical end, Centre - Coarse Grain Coffee used to pick up a pen by the cylindrical end, Right - Fine Grain Coffee used to pick up a pen from a bucket of water by the cylindrical end



Figure 80: Left - Fine Grain Coffee used to pick up a watch, Centre - Coarse Grain Coffee used to pick up a watch, Right - A mixture of Fine & Coarse Grain Coffee used to pick up a watch

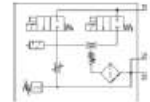
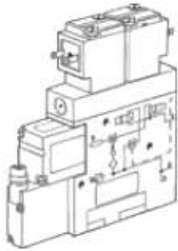
Appendix 7 – Datasheet for Festo Vacuum Generator, VADMI-45-LS-P

Vacuum generator VADMI-45-LS-P

Part number: 171053

FESTO

With air-saving circuit and plug sockets with cable



Data sheet

Feature	values
Nominal size, Laval nozzle	0.45 mm
Assembly position	Any
Ejector characteristic	High vacuum
Integrated function	Ejector pulse valve, electrical Flow control valve Electrical on-off valve Filter Air-saving circuit, electrical Non-return valve Vacuum switch
Design structure	T-shaped
Operating pressure	1.5 ... 8 bar
Max. vacuum	85 %
Duty cycle	100%
Operating medium	Compressed air in accordance with ISO8573-1:2010 [7:4:4]
Note on operating and pilot medium	Lubricated operation not possible
CE mark (see declaration of conformity)	to EU directive for EMC
Medium temperature	0 ... 60 °C
Protection class	IP65
Ambient temperature	0 ... 50 °C
Authorisation	RCM Mark c UL us - Recognized (OL)
Product weight	90 g
Electrical connection	Plug
Mounting type	with through hole with internal (female) thread Optional
Pneumatic connection, port 1	M5
Pneumatic connection, port 3	Non-ducted
Vacuum connection	M5
Materials note	Free of copper and PTFE
Materials information, housing	Aluminium

Appendix 8 – Datasheet for Festo Pneumatic Accessories

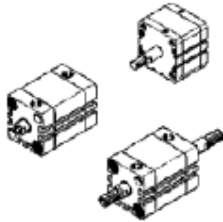
8.1. Festo linear piston (ADN-12-250-APA)

Compact cylinder

ADN-12- -

Part number: 536203

For position sensing, with male or female thread on the piston rod.



Data sheet

Feature	values
Stroke	1 ... 300 mm
Piston diameter	12 mm
Based on the standard	ISO 21287
Cushioning	P: Flexible cushioning rings/plates at both ends
Assembly position	Any
Design structure	Profile barrel Piston rod Piston
Position detection	For proximity sensor
Variants	Single-ended piston rod laser etched rating plate Heat resistant seals, max. 120°C Through piston rod Low-friction Constant slow movement Excellent corrosion protection With protection against rotation Extended piston rod special thread on piston rod Extended male piston rod thread EX protection approval (ATEX)
Operating pressure	1 ... 10 bar
Mode of operation	double-acting
ATEX category Gas	II 2G
Explosion ignition protection type Gas	c T4
ATEX category Dust	II 2D
Explosion ignition protection type Dust	c 120°C
Explosion-proof ambient temperature	-20°C ≤ Ta ≤ +60°C
Operating medium	Compressed air in accordance with ISO8573-1:2010 [7:4:4]
Note on operating and pilot medium	Lubricated operation possible (subsequently required for further operation)
CE mark (see declaration of conformity)	to EU directive explosion protection (ATEX)
Corrosion resistance classification CRC	2
Ambient temperature	-20 ... 120 °C
Theoretical force at 6 bar, return stroke	51 N
Theoretical force at 6 bar, advance stroke	51 ... 68 N
Mounting type	with internal (female) thread with through hole Optional with accessories
Pneumatic connection	M5
Materials note	Conforms to RoHS
Materials information for cover	Anodised Aluminium
Materials information for piston rod	High alloy steel
Materials information for cylinder barrel	Wrought Aluminium alloy Smooth anodised

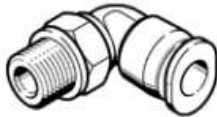
8.2. Festo Plastic Tubing PAN-6X1-NT



Data sheet

Feature	values
Delivery date:	→ View
Outside diameter	6 mm
Bending radius relevant for flow rate	32 mm
Inside diameter	4 mm
Min. bending radius	14 mm
Temperature dependent operating pressure	-0.95 ... 19 bar
Operating medium	Compressed air in accordance with ISO8573-1:2010 [7:-:-]
Ambient temperature	-30 ... 80 °C
Authorisation	TUV
Product weight according to length	0.016 kg/m
Colour	neutral
Shore hardness	D 55 +/-3
Materials note	Free of copper and PTFE Conforms to RoHS
Materials information for tubing	TPE-A

8.3. Push-in fittings: QSM Quick Star L-shape connector QSML-M5-6



Data sheet

Feature	values
Size	Mini
Nominal size	2.1 mm
Type of seal on screw-in stud	Sealing ring
Assembly position	Any
Container size	10
Design structure	Push/pull principle
Operating pressure complete temperature range	-0.95 ... 6 bar
Temperature dependent operating pressure	-0.95 ... 14 bar
Operating medium	Compressed air in accordance with ISO8573-1:2010 [7:-:-]
Note on operating and pilot medium	Lubricated operation possible
Corrosion resistance classification CRC	1
Ambient temperature	-10 ... 80 °C
Authorisation	Germanischer Lloyd
Nominal tightening torque	1.33 Nm
Tolerance for nominal tightening torque	± 20 %
Product weight	4.1 g
Pneumatic connection, port 1	Male thread M5
Pneumatic connection, port 2	For tubing outside diameter 6 mm
Colour of release ring	blue
Materials note	Conforms to RoHS
Materials information, housing	PBT
Release ring material data	POM
Materials information for tubing seal	NBR
Hose clamping segment material data	High alloy steel, non-corrosive

Appendix 9 – Datasheet for O-rings

9.1. End-effector face Seal

O-Ring Division
Parker

Face Seal

2-151
O-Ring Dimensions (mm)

	Nominal	+1/-0
Inner Diameter (ID)	75.87	0.51
Gross Section (RS)	2.62	0.08

External Pressure, Liquid
Suggested Gland Dimensions

	Nominal	+1/-0	Max
Gland Inner Diameter	75.87	0.76	0.00
Gland Depth (D)	1.96	0.08	0.08
Gland Width (SC)	3.53	0.08	0.08
Male Gap (PG)	0.00	0.00	0.00

Gland dimensions can be customized by clicking on the boxes above.

Resulting Tolerance Stackups

	Min	Max	Min	Max	Total
Result	None	None	1.62%	None	None
Equation	18.69%	25.19%	32.37%	20.92%	20.92%
Volume FR	67.55%	77.55%	86.93%	92.40%	92.40%
SC Interference	None	None	None	0.0%	0.0%

9.2. End-effector radial Seal

O-Ring Division
Parker

Radial Static

2-121
O-Ring Dimensions (mm)

	Nominal	+1/-0
Inner Diameter (ID)	26.54	0.25
Gross Section (RS)	2.62	0.08

Male Static Seal
Suggested Gland Dimensions

	Nominal	+1/-0	Max
Groove Diameter	27.64	0.00	0.05
Groove Width	3.56	0.13	0.00
Plug Diameter	31.70	0.00	0.03
Bore Diameter	31.75	0.05	0.00

Gland dimensions can be customized by clicking on the boxes above.

Resulting Tolerance Stackups

	Min	Max	Min	Max	Total
Result	0.69%	3.75%	6.75%	6.75%	6.75%
Equation	14.81%	19.79%	32.60%	17.34%	17.34%
Volume FR	67.55%	77.55%	77.99%	92.40%	92.40%
Intermittent Clearance	0.05	0.05	0.13	0.0	0.0

9.3. Servo Housing Face Seal

O-Ring Division
Home

Face Seal

2-156
O-Ring Dimensions (mm)

	Nominal	Actual
Inner Diameter (ID)	107.62	0.76
Outer Diameter (OD)	2.82	0.08

External Pressure, Liquid
Suggested Gland Dimensions

	Nominal	High	Low
Gland Inner Diameter	107.99	1.07	0.00
Gland Depth (D)	1.90	0.08	0.08
Gland Width (G)	3.53	0.08	0.08
Flare Gap (F)	0.00	0.00	0.00

Gland dimensions can be customized by clicking on the boxes above.

Resulting Tolerance Stackups

	Min	Sum	Max	Total
Inner ID	None	0.30%	2.00%	None
Inner OD	16.54%	25.18%	31.27%	20-30%
Outer ID	87.22%	77.02%	88.94%	80-90%
OD Tolerance	None	None	None	0-5%

Appendix 10 – Table 5: Tabulation of Results of Gripping Various Weights using a 24” Jamming Gripper

Object No.	Tested Object (Weight / Dimensions)	24” Balloon Outcome
1	Cylindrical K’nex structure (49g / width = 5.9 mm)	100% success
2	Hemispherical Optical Mouse (55g / width = 48.4mm)	100% success
3	Cylindrical PVC pipe (118g/ diameter = 25 mm)	100% success
4	Cylindrical PVC pipe (221g/ diameter = 32 mm)	100% success
5	T-junction PVC pipe (103g/ diameter = 40 mm)	80% success
6	Cylindrical PVC pipe (142g/ diameter = 43mm)	70% success
7	Cylindrical PVC pipe (274g/ diameter = 25 mm)	40% success
8	Cuboid Power Bank (350g / width = 60.4 mm)	20% success
9	Cylindrical PVC pipe (447g/ diameter = 43 mm)	20% success

Video Link can be obtained from <https://www.dropbox.com/s/2cgnems5uyp06dd/Air%20Gripper.avi?dl=0>

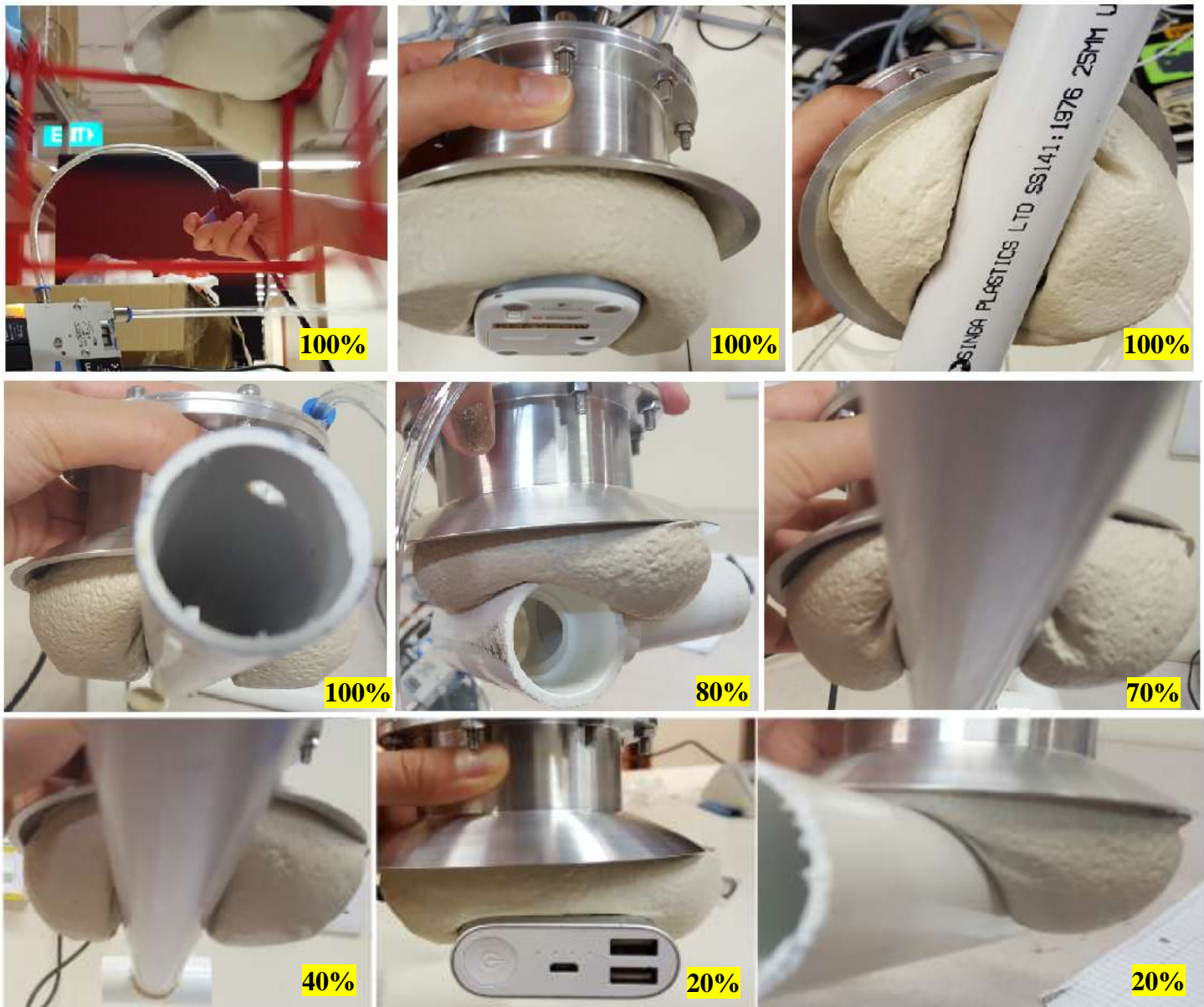


Figure 81: Gripping of Various Objects in air trials; First row (from left) – K'nex structure, Optical Mouse, 25mm cylindrical light PVC pipe; Second Row (from left) – 32mm cylindrical PVC pipe, T-junction PVC pipe, 43mm cylindrical light PVC pipe; Third Row(from left) - 25mm cylindrical heavy PVC pipe, cuboid power bank, 43mm cylindrical heavy PVC pipe

Appendix 11: Servo Datasheet and Torque Calculations

Detailed Specifications

Control System: +Pulse Width Control 1500usec Neutral
Required Pulse: 3-5 Volt Peak to Peak Square Wave
Operating Voltage Range: 4.8-7.4 Volts
Operating Temperature Range: -20 to +60 Degree C (-4F to +140F)
Operating Speed (4.8V): 0.18 sec/60° at no load
Operating Speed (6.0V): 0.15 sec/60° at no load
Operating Speed (7.4V): 0.13 sec/60° at no load
Stall Torque (4.8V): 344oz/in. (22kg.cm)
Stall Torque (6.0V): 402oz/in. (29kg.cm)
Stall Torque (7.4V): 486oz/in. (35kg.cm)
Operating Angle: 45 Deg. one side pulse traveling 400usec
Continuous Rotation Modifiable: Yes
Direction: Clockwise/Pulse Traveling 1500 to 1900usec
Idle Current Drain (4.8V): 9mA at stop
Idle Current Drain (6.0V): 9mA at stop
Current Drain (4.8V): 220mA/idle and 3.8 amps at lock/stall
Current Drain (6.0V): 300mA/idle and 4.8 amps at lock/stall
Dead Band Width: 1usec
Motor Type: Coreless Carbon Brush
Potentiometer Drive: 6 Slider Indirect Drive
Bearing Type: Dual Ball Bearing MR106
Gear Type: Titanium Gears
Connector Wire Length: 11.81" (300mm)
Dimensions: 1.57" x 0.79"x 1.50" (40 x 20 x 38mm)
Weight: 2.40oz (68g)



Figure 82: HS-7950TH Servo Specifications (Servocity, 2016)

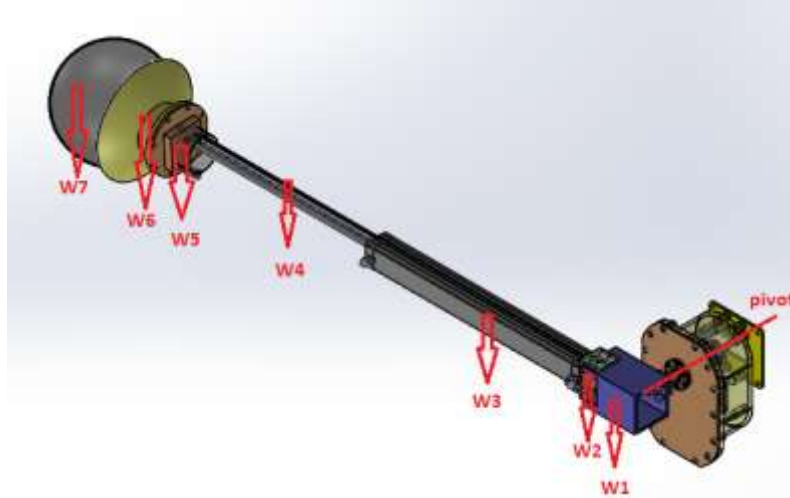


Figure 83: CAD Model of Manipulator Arm

- **Torque = weight (W) x perpendicular distance (d) from pivot**
- Assumptions made: Contribution from the weight of pneumatic tubes, bolts and nuts are taken to be negligible; a safety factor is incorporated; All components are assumed to be uniform; servo housing and accessories are along the line of pivot and have no added effect on torque (Weight = 441.49g);

g taken to be 9.81m/s^2

Total Weight of Manipulator = $\sum W = 1085.08 + 441.49 = 1526.57 \text{ g}$

Link 1 **W1**= 52.03 g, **d1** = 19.55 mm

Actuator support **W2** = 17.24 g, **d2** = 55.27 mm

Linear Piston inclusive of push-in fittings **W3** = 379g, **d3** = 205.59 mm

Guide Rod **W4** = 21.45g, **d4** = 442.26mm

EE support **W5** = 107.51g, **d5** = 611.58mm

EE Collar **W6** = 207.85 g, **d6** = 641.39 mm

EE Membrane **W7** = 300 g, **d7** = 702 mm

Stall Torque = $(52.03 \times 19.55 + 17.24 \times 55.27 + 379 \times 205.59 + 21.45 \times 442.26 + 107.51 \times 611.58 + 207.85 \times 641.39 + 300 \times 702) \times 9.81 / 1000 \times 1000 = 4.90 \text{ Nm}$

Motor selected: HS 7950TH, max torque = 17.16 Nm

Max weight that can be lifted with 7.4V power ~1.78 kg in air

Table 6: Tabulation of Stepped-Up Servo HS-7950TH Characteristics

HS7950TH (5:1 ratio)	Imperial Units	Metric Units
Dimensions:	1.57" x 0.79"x 1.50"	40 x 20 x 38mm
Weight:	2.40oz	68g
Max angle of Rotation	180°	
Stall Torque:		
4.8V Power	1720 oz-in	12.15 Nm
6.0V Power	2010 oz-in	14.19 Nm
7.4V Power	2430 oz-in	17.16 Nm
Operating Speed		
4.8V Power	0.9 sec/60° = 11.1 rpm	
6.0V Power	0.75 sec/60° = 13.3 rpm	
7.4V Power	0.65 sec/60° = 15.4 rpm	

Appendix 12: Datasheet for 6.4x9x16 TUCRT Spring Energised Rotary Seal from Advanced Sealing Devices



Specifications

Temperature	-60 ^o C up to 200 ^o C, depending on materials
Media	Hydraulic, lubricating and mineral oil based on lubricating greases, HFA, HFB, HFC; contact us for other media
Velocity	< 5 m/s
Pressure	< 200 bar

Materials Available

Materials		Operating Temp °C
Poly tetra fluoro ethylene	PTFE	-200 to 250
PTFE glass filled	PTFE-Glass	-200 to 250
PTFE graphite filled	PTFE-Graphite	-200 to 250
PTFE carbon filled	PTFE-Carbon	-200 to 250
PTFE bronze filled	PTFE-Bronze	-200 to 250
PTFE glass and Moly filled	PTFE-Glass-MoS2	-200 to 250
Polyethylene	UHMW-PE	-200 to 120

Materials (O-Ring)		Operating Temp °C
Nitrile Rubber	NBR	-45 to 120
Nitrile, hydrogenated	HNBR	-20 to 150
Ethylene Propylene diene	EPDM	-45 to 150
Fluorocarbon	FKM	-15 to 200
Silicone	VMQ	-60 to 200

Appendix 13: Images from Water Trials on Gripped Items



Figure 84: Gripping of Various Objects in air trials; First row (from left) – 25mm PVC Pipe, 43mm PVC Pipe, K'nex Structure, Second Row (from Left): U channel, Odd Geometric Structure, Square tube, Sphere ,Third Row (from left): 2 Pearl Weight, Screwdriver Head, Kick Board

Video Link can be obtained from <https://www.dropbox.com/s/uikm1ps8tq9rj9v/Water%20full%201.avi?dl=0>

References

- Anaheimautomation.com,. (2015). *AC Motors, Controllers, and Variable Frequency Drives*. Retrieved 31 December 2015, from <http://www.anaheimautomation.com/manuals/forms/ac-motor-guide.php#sthash.rdM5viNL.dpuf>
- Amend, J., Brown, E., Rodenberg, N., Jaeger, H., & Lipson, H. (2012). A Positive Pressure Universal Gripper Based on the Jamming of Granular Material. *IEEE Transactions on Robotics*, 28(2), 341–350.
<http://doi.org/10.1109/TRO.2011.2171093>
- Bouchard, S. (2015). *Top 5 Advantages of Servo-Electric Grippers*. *Blog.robotiq.com*. Retrieved 31 December 2015, from <http://blog.robotiq.com/bid/37840/Top-5-Advantages-of-Servo-Electric-Grippers>
- Brown, E., Rodenberg, N., Amend, J., Mozeika, a., Steltz, E., Zakin, M. R., ... Jaeger, H. M. (2010). From the Cover: Universal robotic gripper based on the jamming of granular material. *Proceedings of the National Academy of Sciences*, 107(44), 18809–18814. <http://doi.org/10.1073/pnas.1003250107>
- Brighthub Engineering,. (2015). *Robotics: Structure of Industrial Robots or Manipulators: Types of Base Bodies - I*. Retrieved 5 December 2015, from <http://www.brighthubengineering.com/robotics/26371-robotics-structure-of-industrial-robots-or-manipulators-types-of-base-bodies-one/>
- Circuitdigest.com,. (2015). *What are industrial manipulators - Different Types of Industrial Manipulators*. Retrieved 5 December 2015, from <http://circuitdigest.com/article/what-are-industrial-manipulators>
- Coastalwiki.org. (2016). *Currents - Coastal Wiki*. Retrieved 10 April 2016, from <http://www.coastalwiki.org/wiki/Currents>
- Control Design,. (2015). Festo's DHxS Gripper Series. Retrieved 31 December 2015, from

<http://www.controldesign.com/vendors/products/2012/festo-dhxs-gripper-series/>

Cooney, L. A. (2006). *Development of a Low-Cost Underwater Manipulator*. Massachusetts Institute of Technology.

Design Aerospace. (2016). *Gears*. Retrieved 1 March 2016, from

<http://www.daerospace.com/MechanicalSystems/GearsDesc.php>

Follmer, S., Leithinger, D., Olwal, A., Cheng, N., & Ishii, H. (2012). Jamming User Interfaces: Programmable Particle Stiffness and Sensing for Malleable and Shape-Changing Devices. *Proceedings of the 25th Annual ACM Symposium on User Interface Software and Technology - UIST '12*, 519–528.

<http://doi.org/10.1145/2380116.2380181>

Herman, A. (2013). Shear-jamming in two-dimensional granular materials with power-law grain-size distribution. *Entropy*, 15(11), 4802–4821. <http://doi.org/10.3390/e15114802>

Hyperphysics,. (2015). *Bernoulli Equation*. Retrieved 15 December 2015, from <http://hyperphysics.phy-astr.gsu.edu/hbase/pber.html>

Ikont.co.jp,. (2016). *IKO Standard Type Cam Follower CF / Products / IKO NIPPON THOMPSON*. Retrieved 1 January 2016, from <http://www.ikont.co.jp/eg/product/needle/ndl0601.html>

Industrial Circuits Application Note,. (2015). *Stepper Motor Basics*. Retrieved 31 December 2015, from <http://www.solarbotics.net/library/pdflib/pdf/motorbas.pdf>

Jacobsanalytics.com,. (2016). *Venturi eductors or vacuum pumps*. Retrieved 1 January 2016, from <http://jacobsanalytics.com/eductors/venturi-eductors/>

Kuttan, A. (2007). *Robotics*. New Delhi: I.K. International Publishing House.

- Misumi,. (2016). *CFFAP6-16 / Cam Followers/Solid Eccentric / MISUMI / MISUMI*. *Uk.misumi-ec.com*. Retrieved 1 January 2016, from <http://uk.misumi-ec.com/vona2/detail/110302644810/?HissuCode=CFFAP6-16>
- Mozeika, A. (2015). *Granular Jamming*. Retrieved 1 February 2016, from <http://www.annan.io/articles/54>
- Nair, P. (2009). *Types of Artificial Gripper Mechanisms - Society of Robotics & Automation*. Available at: <http://sra.vjti.info/knowledgebase/posts-on-a-roll-1/gripper-mechanisms>
- Omron. (2016). *Subminiature Basic Switches (S-Size)*. Retrieved 1 March 2016, from <https://www.omron.com/ecb/products/sw/12/ss.html>
- Parker. (2006). *Rotary Seal Design Guide*.
- Parker FAQ. (2016) (1st ed.). Retrieved 1 March 2016, from <http://www.parker.com/Literature/O-Ring%20Division%20Literature/FAQ.pdf>
- Pololu.com,. (2015). *Pololu - Stepper Motor: Bipolar, 200 Steps/Rev, 20×30mm, 3.9V, 0.6 A/Phase*. Retrieved 31 December 2015, from <https://www.pololu.com/product/1204>
- Ridao, P., Carreras, M., Ribas, D., Sanz, P. J., & Oliver, G. (n.d.). *Intervention AUVs : The Next Challenge*.
- RobotWorx, (2015). *Grippers For Robots*. Retrieved 31 December 2015 from <https://www.robots.com/articles/viewing/grippers-for-robots>
- RS Components. (2016). *Optek OPB815WZ Chassis Mount Slotted Optical Switch, Phototransistor Output*. Retrieved 1 March 2016, from <http://sg.rs-online.com/web/p/slotted-optical-switches/1944030/>
- Sapagroup.com,. (2016). *Aluminum U Channel / Sapa Extrusions North America / Sapa Group*. Retrieved 1 January 2016, from <http://www.sapagroup.com/en/na/profiles/aluminum-u-channel/>

Seabotix,. (2015). *SeaBotix Inc. Grabber Attachments*. Retrieved 5 December 2015, from

http://www.seabotix.com/products/grabber_attachments.htm

Servocity.com,. (2016). *Servo Shaft Hub (.500")*. Retrieved 1 January 2016, from

https://www.servocity.com/html/servo_shaft_hub_500_.html#.VoX15fl97IU

Tetrixrobotics.com,. (2015). *180° Standard-Scale HS-485HB Servo Motor (W39197)*. Retrieved 31 December

2015, from http://www.tetrixrobotics.com/180_Standard-Scale_HS-485HB_Servo_Motor

Tigertek Industrial Services,. (2015). *How Actuators Work - Basic Actuators for Motion Control*. Retrieved 31

December 2015, from <http://www.tigertek.com/servo-motor-resources/how-actuators-work-in-motion-control.html>

Vacuum cups, suction cups and suction pads. (2016). Fipa.com. Retrieved 4 February 2016, from

http://www.fipa.com/en_GB/products/212414-vacuum-cups

Xu, N., & Ching, E. S. C. (2010). Effects of particle-size ratio on jamming of binary mixtures. *The Royal*

Society of Chemistry 2010, 5. <http://doi.org/10.1039/b926696h>